Unraveling short-and long-term carbon cycle variations during the Oceanic Anoxic Event 2 from the Paris Basin Chalk

Slah Boulila, Guillaume Charbonnier, Jorge Spangenberg, Silvia Gardin, Bruno Galbrun, Justine Briard, Laurence Le Callonnec

Global and Planetary Change, Volume 186, March 2020, 103126.
https://doi.org/10.1016/j.gloplacha.2020.103126

Unraveling short- and long-term carbon cycle variations during the Oceanic Anoxic Event 2 from the Paris Basin Chalk

Slah Boulila[ab], Guillaume Charbonnier[ac], Jorge E. Spangenberg[d], Silvia Gardin[e], Bruno Galbrun[a], Justine Briard[a], Laurence Le Callonnec[a]

[a] Sorbonne Université, CNRS-INSU, Institut des Sciences de la Terre Paris, ISTEP UMR 7193, F-75005 Paris, France
[b] ASD/IMCCE, CNRS-UMR 8028, Observatoire de Paris, PSL University, Sorbonne Université, 77 Avenue Denfert-Rochereau, 75014 Paris, France
[c] Institute of Earth Sciences, University of Lausanne, Géopolis, CH-1015 Lausanne, Switzerland
[d] Institute of Earth Surface Dynamics, University of Lausanne, Géopolis, CH-1015 Lausanne, Switzerland
[e] Sorbonne Université, MNHN, CNRS, Centre de Recherche sur la Paléobiodiversité et les Paléoenvironnements, CR2P, F-75005 Paris, France

Received 28 August 2019,
Revised 8 January 2020,
Accepted 15 January 2020
Available online 20 January 2020.

Keywords
OAE2
Paris Basin
Volcanism
Carbon cycle
Eccentricity amplification
CTB
Diachroneity

Abstract
The Oceanic Anoxic Event 2 (OAE2, ca. 94.6 Ma) is one of the major perturbations in the global carbon cycle during the Phanerozoic. Stable carbon isotopes ($\delta^{13}C$) from marine and continental sedimentary environments document this carbon cycle perturbation with a pronounced (> 2‰) positive carbon isotope excursion (CIE). Although the OAE2 stratigraphic interval has been intensively studied in terms of paleoceanography and paleoclimatology, several climatic and carbon cycle aspects are not yet well-understood. In particular, cyclic short-term Milankovitch-scale $\delta^{13}C$ variations within the OAE2 and their potential implications for the global carbon cycle have been rarely addressed. Here, we present high-resolution (5 cm, ~2 kyr) $\delta^{13}C$ data spanning the OAE2 from the Paris Basin Chalk (Poigny Craie-701 drill-core) to show high amplitude short-term $\delta^{13}C$ oscillations, superimposed on the major CIE. Time-series analysis indicates that short-term oscillations are astronomically paced, with eccentricity cycles being the most prominent. Orbital forcing of $\delta^{13}C$ variations is further supported by time-series analysis of the English Chalk (Eastbourne section). We suggest that orbitally paced carbon cycle oscillations were amplified by considerable emission of greenhouse gases from volcanism that caused the overall CIE. Astronomical calibration of the whole OAE2 (the perturbation and recovery

phases) from the Poigny record provides a duration equivalent to eight to eight and a half short eccentricity cycles.
Cyclostratigraphic correlations among several OAE2 key records indicate the same duration of the whole CIE. However, duration of the interval from the onset of CIE till the Cenomanian-Turonian boundary (CTB) is significantly different from one basin to another. In particular, a difference of almost two short eccentricity cycles is highlighted between the Anglo-Paris and Western Interior basins. According to cyclostratigraphic approach and correlations, the entry of *W. devonense* was at least 200 kyr later in the Western Interior Basin (WIB, USA) than in Europe. Key calcareous nannofossil biohorizons (e.g., *Quadrum gartneri*) are also stratigraphically upshifted in the WIB with respect to the European sections, hence concurring with the hypothesis of a younger CTB in the WIB. We ascribe such significant temporal offset to diachroneity of the CTB, which is likely the result of different, regional biotic responses to the global OAE2 paleoenvironmental perturbation.

1. Introduction

During the time interval spanning the Late Cenomanian-Early Turonian, the Earth experienced severe global warming (e.g., Huber et al., 2002; Voigt et al., 2004) associated with profound perturbations of the ocean-continent and biosphere systems. The cause of these changes is most commonly attributed to intense volcanic eruptions from Large Igneous Provinces widespread on Earth during this time interval, resulting in excessive and rapid influx of carbon dioxide (CO_2) into the atmosphere and hydrosphere systems (Jenkyns, 2010). This may have induced global climate change, disturbances in the biotic and geochemical cycles, and the onset of widespread ocean anoxia during the critical geological event, known as Oceanic Anoxic Event 2 (OAE2, Schlanger and Jenkyns, 1976). Deep sea environments during the OAE2 witnessed extraordinary enhanced nutrient availability and dramatic decrease in dissolved oxygen concentrations. This led to unusual organic productivity and accumulation of organic matter in ocean sediments and the formation of black shale or organic-rich intervals, which constitute today major petroleum source rocks worldwide (Haq et al., 1987). Fossil and geochemical sedimentary proxies from multiple sites in oceans and continents highlight these severe changes in the biogeochemical cycles. In particular, stable carbon isotopes ($\delta^{13}C$) in carbonate and organic sediments indicate a salient perturbation in the global carbon cycle, expressed as a pronounced, short-lived (< 1 Myr) positive carbon isotope excursion (CIE) (e.g., Scholle and Arthur, 1980; Gale et al., 1993; Paul et al., 1999; Tsikos et al., 2004; Jarvis et al., 2006; Sageman et al., 2006). Thus, marine carbonate and organic CIEs have been used to define the extent of OAE2, since OAE2 organic-rich intervals (or black shale) are not correlatable worldwide (Tsikos et al., 2004; Erbacher et al., 2005; Jarvis et al., 2006; Voigt et al., 2008).
Pronounced short-term oscillations within the OAE2 from multiple paleoclimatic and paleoceanographic data proxies have been studied in detail. For instance, short-term (Milankovitch scale) oscillations in organic-matter proxy (total organic carbon), as well as those in continental weathering proxies have been investigated to better understand the mechanisms behind enhancement of organic matter accumulation and/or preservation and the impact of OAE2 on the hydrological cycle (e.g., Meyers et al., 2012a; Poulton et al., 2015; Charbonnier et al., 2018).
The CIE exhibits prominent internal, short-term $\delta^{13}C$ variations (Pratt, 1985; Gale et al., 1993; Erbacher et al., 2005; Jarvis et al., 2006; Voigt et al., 2008; Elrick et al.,

2009, e.g., $\delta^{13}C$ peaks A, B and C; negative $\delta^{13}C$ Plenus Cool Event), which have been rarely explored in terms of Milankovitch forcing, and their record requires highly-resolved $\delta^{13}C$ data (Li et al., 2017).
Here, we present new high-resolution (~2 kyr) carbonate $\delta^{13}C$ data from the Paris Basin Chalk, able to capture the high-frequency Milankovitch band. The three main objectives of the study were to: (i) characterize with high fidelity the CIE, (ii) study with higher resolution short-term $\delta^{13}C$ oscillations within the CIE and their potential astronomical origin, and (iii) discuss the duration of OAE2.

2. Material and methods

2.1. Material

2.1.1. Lithostratigraphy and stable carbon isotopes

"Poigny-CRAIE 701" drill-core in the Paris Basin (Fig. 1) covers almost 700 m thick sedimentary sequence of most of the Late Cretaceous Epoch (Mégnien and Hanot, 2000). We studied a ~41 m thick stratigraphic interval spannig the OAE2 (Fig. 2). Lithostratigraphy and biostratigraphy (planktonic foraminifera and calcareous nannofossils) were first presented by Janin (2000), Robaszynski (2000), Robaszynski and Bellier (2000) and later by Robaszynski et al. (2005), but still with lower resolution, as these previous studies were carried out on the entire drill-core (Mégnien and Hanot, 2000). Here, we updated the lithological description and revised calcareous nannofossil biostratigraphy within the OAE2 interval (Section 2.1.2).
Lithology is composed of marl, limestone to chalk (Fig. 2) including the main features of OAE2 interval observed in the English Chalk, such as the Plenus Cooling Event (Gale and Christensen, 1996).
The interval from 632 to 660 m was sampled with high resolution, every 5 cm. Bulk carbonate stable carbon isotope ratios ($\delta^{13}C$) were measured in all samples at the University of Lausanne, using a Thermo Fisher Scientific (Bremen, Germany) Gas Bench II carbonate preparation device connected to a Delta Plus XL isotope ratio mass spectrometer. The $\delta^{13}C$ values are expressed in per mil relative to the Vienna PDB (V-PDB) standard. Precision of $\delta^{13}C$ measurements, estimated as the standard deviation of the mean calculated for replicate analyses of international standards NBS 18 and NBS 19, and the laboratory standard Carrara Marble, is ±0.05‰.

2.1.2. Calcareous nannofossil biostratigraphy

Calcareous nannofossil biostratigraphy was analyzed each 1 m through the studied interval using a Zeiss Axioscope imaging II at 1500 × using cross-polarized and plane light. Core samples were processed to observe calcareous nannofossils in simple smear slides using ammonia water (pH = 8.5) in order to prevent dissolution. Three traverses were thoroughly examined to locate and quantify key biostratigraphic taxa.
Calcareous nannofossils are relatively few to common and overall poorly preserved. This poor preservation is mainly due to fragmentation (compaction) of calcareous nannofossils rather than dissolution and etching.
The available nannofossil zonation schemes are not always applicable because there are significant differences in the stratigraphic succession of nannofossil biohorizons reported by different authors. This diachroneity can be real if it is due to the paleoenvironmental perturbation, and paleoecologic and paleogeographic positions

of the sections. It could be apparent if it is due to preservation artefacts and/or discrepant taxonomic concepts among researchers. Other factors play a role in the reproducibility and reliability of the biohorizons, expanding the confidence interval of the appearance/disappearance datum resulting in (apparent) diachroneity: rare occurrences at the beginning/end of species ranges, due to reworking or changing sedimentation rates among the sections. Discrepant analytical approaches (qualitative vs. quantitative logging and time spent at the microscope) might also play a role.

In this work, we preferred to focus on occurrences of biohorizons and their positions against the $\delta^{13}C$ curve rather than the establishment of biozonation based on a biostratigraphic scheme. Thus, the sequence of calcareous nannofossil biohorizons based on 1 m sampling space is shown in Fig. 2A. They are the most important key taxa that usually constrain the Cenomanian-Turonian boundary (CTB) interval (Fig. 2A and Plate S1) and their vertical succession is more or less comparable to previous studies across the CTB interval in other boreal sections (Paul et al., 1999; Linnert et al., 2011), as well as low-latitude Tethyan sections (Tsikos et al., 2004; Hardas and Mutterlose, 2006; Fernando et al., 2010). The discrepancies are mainly due to aforementioned factors.

Biohorizons, which have been used as good indicators of the CTB are the Top (highest occurrence or last occurrence) of *Helenea chiastia* (upper part of Plateau before peak 'C'), and the Base (lowest occurrence or first occurrence) of *Quadrum gartneri* (beginning of recovery), as already suggested in previous studies (Tsikos et al., 2004; Desmares et al., 2007; Hardas and Mutterlose, 2006; Fernando et al., 2010). A precise $\delta^{13}C$ correlation with the Eastbourne (UK) reference section allows the CTB at Poigny to be refined (Section 4.1). Linnert et al. (2011) reported a slightly earlier occurrence of *Q. gartneri* in England (end of Plateau). The Top of *Lithraphidites acutum* and *Axopodorhabdus albianus* and Base of *Rotelapillus biarcus* can help to refine the biostratigraphic framework. However, *L. acutum* is impacted by fragmentation and it is rare at the end of its stratigraphic range in the Poigny core. It has been recognized only till the depth of 653.90 m, making this species less reliable as a biostratigraphic marker. The Top of *Corollithion kennedyi* and *A. albianus* are younger in other sections (Linnert et al., 2011) and it is difficult to prove reworking versus true diachronous extinction. *Cretarhabdus loriei* has been found only sporadically in Poigny core and thus is not reported as a key marker.

2.2. Methods

$\delta^{13}C$ data were described and correlated to previous $\delta^{13}C$ records (Section 4.1), and then submitted to spectral analysis via the multitaper method (MTM, Thomson, 1982) to seek cyclicities. The MTM spectra were conducted using three 2π tapers, together with the robust red noise test (Mann and Lees, 1996) as implemented in the R package 'astrochron' freeware (Meyers, 2014). Prior to spectral analysis, the data were detrended using the weighted-average lowess method (Cleveland, 1979). We used smoothing low-pass filtering based on the Savitzky-Golay (S-G) method (Savitzky and Golay, 1964) in order to highlight both short- and long-term $\delta^{13}C$ variations (Fig. 2B). This method has the potential to filter out a large frequency band from an oversampled signal corrupted by noise, and has the advantage of preserving several variabilities, as well as the width and height of waveform peaks (Savitzky and Golay, 1964). The $\delta^{13}C$ data are noisy and preserve high- and low-frequencies as well as the overall CIE. Thus, to isolate all these variations, we applied the S-G filter

(Fig. 2B, C, D). We also used the gaussian filter (Paillard et al., 1996) to extract the recorded astronomical cycles. The tuning was performed on the basis of the dominant short eccentricity cycle because it is the dominant orbital parameter (with the greatest noise-to-signal ratio, Fig. 3) and its mean period is more reliable than precession and obliquity mean components (e.g., Laskar et al., 2004).

3. Results

The $\delta^{13}C$ values shift from 2.7 to 5.2‰ at the onset of OAE2, recording the CIE with an amplitude of 2.5‰ (Fig. 2B). This amplitude and relative $\delta^{13}C$ variations are very similar to those documented in the English Chalk (Paul et al., 1999; Jarvis et al., 2006). A detailed correlation between Poigny core and other OAE2 key $\delta^{13}C$ records, including the English Chalk, is provided in Fig. 4, Fig. 5 and Supplementary Fig. S1. Prominent shorter term $\delta^{13}C$ fluctuations superimposed on the CIE could be observed in the highly-resolved Poigny data, quantified below via spectral analysis.

Spectral analysis of carbon isotope data (Fig. 3) shows a strong peak centered on a period of 2.94 m. Four other significant peaks, but with lower powers, are characterized by periods of 1.03, 0.63 and 0.38 m. Finally, two non-significant peaks are centered on periods of 0.46 and 0.26 m. Frequency ratio of 1.03/2.94 falls in the range of the fundamental obliquity period over the mean period of short eccentricity (37.3 kyr over 110 kyr, Laskar et al., 2004). Frequency ratios of 0.63/2.94 and 0.46/2.94 fall in the order of the precession periods over the mean short eccentricity period (P1: 21.9 kyr, P2: 18.4 kyr over 110 kyr, Laskar et al., 2004). Thus, we interpreted the peaks 2.94, 1.03, 0.63 and 0.46 m as reflecting, respectively, short eccentricity (100 kyr), obliquity (O1), and precession components (P1 and P2). The 0.38 m peak may correspond to the shortest precession component (P3: 15.9 kyr, Laskar et al., 2004), while 0.26 m peak may represent a sub-Milankovitch frequency.

Then, we tuned the 2.94 m $\delta^{13}C$ wavelength to a mean short eccentricity period of 100 kyr. Such tuning allows calibration of ~1 m wavelength to a period of 36.1 kyr, matching the obliquity frequency band. The 0.63 m peak was calibrated to 22.5 kyr, which would represent a longer precession component. Finally, the wavelengths of 0.46 and 0.38 m were tuned to 16.5 and 13.9 kyr, which would represent shorter precession components.

We then used the 100 kyr $\delta^{13}C$ timescale to infer the duration of OAE2. This requires a consistent definition of the CIE with respect to previous studies. The onset of CIE is commonly replaced at the start of the first significant shift in $\delta^{13}C$ profile. However, the placement of the end of CIE differs from one study to another (Fig. 4).

Poigny record exceptionally captures stratigraphic intervals before, within and after the CIE (Fig. 2B). We defined the extent of CIE from Poigny; then after a detailed correlation with previous $\delta^{13}C$ records, we defined in the same manner the extent of CIE in all sections. The OAE2 at Poigny encompasses eight to eight and a half short eccentricity cycles, providing a duration ranging from ~800 to ~850 kyr (Fig. 2, Fig. 3).

Below, we (i) compare our estimate with previous studies, and (ii) discuss the potential link between the record of prominent short eccentricity cycles and volcanic pacemaker of the overall CIE.

4. Discussion

4.1. Correlation of OAE2 equivalent records: a critical overview

Poigny CIE trends are very similar to those recorded at Eastbourne section (southern England), and share some features with several CIE key records in other basins (Fig. 4, Fig. 5, and Supplementary Fig. S1). Correlations between OAE2 sections have generally been established on the basis of integrated stratigraphy (e.g., Gale et al., 1993, Gale et al., 2018; Jarvis et al., 2006; Sageman et al., 2006; Elrick et al., 2009; Meyers et al., 2012b). Most of OAE2 studied sections come from pelagic to hemipelagic settings, although nearshore marine setting can preserve the OAE2 with high fidelity. For instance, the Morelos Formation of shallow-water platform carbonates in southern Mexico captures the OAE2 interval with a thickness of >50 m (Elrick et al., 2009), compared to only ~34 m at the hemipelagic Gongzha section in China (Li et al., 2017), or ~6.75 m and ~2.3 m at the Portland and Gubbio pelagic sections in USA and Italy, respectively (Sageman et al., 2006; Tsikos et al., 2004). We established a correlation between cyclostratigraphically studied key sections from three basins (Fig. 4), the Anglo-Paris Basin (APB), the Western Interior Basin (WIB), USA, and the northern margin of Indian plate. We used the following criteria: (i) the $\delta^{13}C$ profile, (ii) key biostratigraphic datum levels, (iii) lithostratigraphic markers in the APB, and (iv) bentonite layers and bed markers for sections from the WIB (Fig. 4). Below, we provide a critical overview of the use of some of the aforelisted criteria for OAE2 correlation. For writing simplification, we use the definition of OAE2 extent as the extent of the CIE even though OAE2 would represent facies expression of ocean anoxia.

A first-order correlation of the recorded CIE associated to OAE2 between sections is generally easy to perform. However, a detailed fine correlation at the scale of small $\delta^{13}C$ oscillations is difficult to realize because of the different sampling resolutions and/or the differential preservation of small-scale $\delta^{13}C$ variations between sections (Fig. 4). The onset of the OAE2 interval is more easily correlatable, which could be defined by the first rapid positive $\delta^{13}C$ shift at Poigny, Eastbourne, Gongzha, Portland, Iona-1 and Angus (Fig. 4, Fig. 5). However, the end of CIE, as well as the main small-scale $\delta^{13}C$ excursions (e.g., Peaks A, B and C) constitute controversial interpretations among authors (4.2 Duration of OAE2 and potential paleoenvironmental implications, 4.3 Volcanic amplification of eccentricity driven carbon cycle).

The Top of the planktonic foraminifera *Rotalipora cushmani* represents a key biostratigraphic datum event, which occurred just above the first $\delta^{13}C$ peak (Peak A), and thus has been widely used as a correlation datum (Keller et al., 2001; Keller and Pardo, 2004; Tsikos et al., 2004). Nevertheless, other studies pointed to the diachroneity of the extinction of *R. cushmani* between sites and basins (e.g., Gale et al., 1993; Desmares et al., 2007). The CTB at the Eastbourne section and USGS♯1 Portland core are marked by the Top of *Neocardioceras juddii* and coincident to the Base of *Fagesia catinus* and *Watinoceras devonense* ammonites (Paul et al., 1999; Kennedy et al., 2000, Kennedy et al., 2005; Gale et al., 1993, Gale et al., 2005; Sageman et al., 2006). The CTB has been generally used as a good marker for correlation between basins, e.g. between the APB and WIB (e.g., Gale et al., 2005).

In the absence of ammonites and standard zonal nannofossils at Gongzha section (Fig. 4), the “filament event” as the product of mass mortality of juvenile bivalves, is considered as a biostratigraphic marker for the CTB (Bomou et al., 2013). Although

some studies pointed to the potential use of the “filament event” for global correlation (e.g., Caron et al., 2006), other studies shed light on its unreliability for correlation, even within the same basin (e.g., Desmares et al., 2007). The stratigraphic position of the CTB at Gongzha section is imprecise (Li et al., 2006; Bomou et al., 2013; Li et al., 2017). It was placed roughly at 62.4 m (Li et al., 2006), and within an uncertainty interval from 60.2 to 67.8 m (Bomou et al., 2013), using in both studies planktonic foraminifera zonation and $\delta^{13}C$ correlation in addition to the “filament event”. Li et al. (2017) placed the CTB at ~51.8 m (Fig. 4). Thus, the CTB at Gongzha cannot be used for a precise correlation with other sections (Section 4.2.2).

The Base of calcareous nannofossil *Quadrum gartneri* is situated at around the CTB in some sections (Robaszynski et al., 1993; Jarvis et al., 2006; Tsikos et al., 2004), and hence used as a good marker to place the CTB in the absence of ammonites (e.g., Tsikos et al., 2004; Linnert et al., 2011). Nevertheless, the Base of *Q. gartneri* in the Poigny core occurs at a higher stratigraphic level than in Eastbourne and at a lower stratigraphic level than in the Wunstorf core (Lower Saxony Basin, Germany) (see Section 2.1.2 and Fig. 2). Calcareous nannofossil biohorizons around the CTB have been shown to be stratigraphically shifted between sections and basins, although a concluding remark in terms of the potential diachroneity of these nannofossil biohorizons was not drawn (e.g., Tsikos et al., 2004; Desmares et al., 2007; Fernando et al., 2010; Corbett et al., 2014). Based on the conjoint $\delta^{13}C$ and cyclostratigraphic correlation that we propose, we have investigated the hypothesis of diachronous key nannofossil biohorizons in Section 4.2.2.

The Base of planktonic foraminifera *Helvetoglobotruncana helvetica* was proven to be diachronous between the WIB, APB, and northern margin of Indian plate sections due to ecological effects (Keller et al., 2004; Caron et al., 2006; Sageman et al., 2006; Desmares et al., 2007; Bomou et al., 2013). Also, Desmares et al. (2007) demonstrated that biohorizons of the three planktonic foraminifera *R. cushmani, W. archaeocretacea,* and *H. helvetica* are diachronous between sections in the same WIB. Additional key correlation levels in the WIB were obtained between USGS♯1 Portland and Angus cores owing to lithostratigraphic bed markers and bentonite layers (Ma et al., 2014) (Fig. 4 and Supplementary Fig. S2). In a recent paper, Falzoni et al. (2018) suggested through exhaustive correlations among reference sections in the world that the appearance of *H. helvetica* and some *Dicarinella* species are diachronous across low to mid-latitude localities. Our cyclostratigraphic correlations among different basins further support the diachroneity of key foraminiferal biohorizons. Placed in a common cyclostratigraphic framework based on short eccentricity cycle numbering within the CIE, significant diachroneity of foraminiferal and nannofossil biohorizons was highlighted between basins (see detail in Section 4.2.2).

From the above overview on biohorizons, neither calcareous nannofossils nor planktonic foraminifera could be used for a robust correlation as they could be diachronous among and within basins (Gale et al., 1993; Keller et al., 2004; Caron et al., 2006; Sageman et al., 2006; Desmares et al., 2007; Bomou et al., 2013). According to the literature, only the CTB is synchronous and hence, can be used as a key stratigraphic level for correlation between sections whenever it is well-defined by ammonites (e.g., Kennedy and Cobban, 1991; Cobban and Scott, 1972; Paul et al., 1999; Gale et al., 2005). Thus, to compare duration of specific intervals within the OAE2, we have relied only on three OAE2: stratigraphic levels, the onset of CIE, the CTB, and the end of CIE.

4.2. Duration of OAE2 and potential paleoenvironmental implications

4.2.1. A revised stratigraphic extent of OAE2

The duration of OAE2 and other events showing a perturbation in the carbon cycle, requires a common definition of the stratigraphic extent of the CIE to make any comparison of duration between studies robust (see Boulila and Hinnov, 2017, for a review). The end of CIE is, in general, difficult to define, making comparison of the whole duration of the CIE between studies implausible. For OAE2, Sageman et al. (2006) raised in detail the difficulty to define the end of CIE from the WIB. Tsikos et al. (2004) performed a $\delta^{13}C$ correlation between several sections in the world by fixing the end of OAE2 at the end of Plateau of stable $\delta^{13}C$ values (Fig. 2D). Jarvis et al., 2006, Jarvis et al., 2011 extended OAE2 into the lowermost part of the Turonian. Voigt et al. (2008) placed the end of OAE2 at almost the same position like Tsikos et al. (2004). Eldrett et al. (2015) positioned the end of OAE2 in the WIB at a much higher stratigraphic level because the CTB is likely higher in this basin than in other basins (see Section 4.2.2), but their option still does not reflect the more likely end of CIE (Fig. 4).

In Fig. 2, we propose a revised stratigraphic extent of the OAE2 in the APB, which considers the CIE in its whole extent. It takes into account the perturbation through the return to normal conditions (or recovery phase). We also propose a simple subdivision of different (two) phases of CIE. The first phase corresponds to the carbon cycle perturbation, which spans the increasing part and the Plateau. This phase was selected in some studies to define the extent of OAE2 (e.g., Tsikos et al., 2004). The second phase corresponds to the return to normal conditions (or recovery phase), which extends from the end of the Plateau, i.e. when $\delta^{13}C$ starts decreasing, till the end of CIE. Our definition of 'recovery' interval is different from previous studies (see Fig. 2). Also, our proposition of the extent of the Plateau is different from previous studies. It extends from peak A through the last peak C, instead of from peak B till C (Fig. 2, e.g. Paul et al., 1999). Our goal of the above proposition of extent of OAE2 and its different phases is motivated by the comparison of cyclostratigraphically inferred durations between basins, and especially their potential implications we discuss in Section 4.2.2.

The Plateau as well as the increasing and decreasing parts of CIE exhibit strong short-term $\delta^{13}C$ oscillations, including the well-known small-scale excursions or peaks A, B and C and the Holywell event (Fig. 2, Jarvis et al., 2006). Cyclostratigraphy of Poigny $\delta^{13}C$ data indicates that these cyclic $\delta^{13}C$ variations are orbitally paced by short eccentricity (Section 3). These orbitally paced $\delta^{13}C$ oscillations are apparently characterized with greater amplitudes within the Plateau, with respect to those spanning the increasing and decreasing parts of CIE. We ascribe this difference in amplitude as the result of strong linear (or parabolic) trends in the increasing and decreasing parts related to CIE, which dominate the signal. In contrast, stable $\delta^{13}C$ values within the Plateau make short eccentricity related $\delta^{13}C$ cycles with apparently greater amplitudes.

To make comparison of durations of the OAE2 meaningful, we tentatively revised the stratigraphic extent of the CIE in different sections in the same manner (Fig. 4, Fig. 5, Section 4.2.2). We first compared the duration of the interval from the onset of CIE to the CTB (Fig. 5). To facilitate writing, we will henceforth call this interval as 'perturbation' interval. The actual 'perturbation' interval should be considered from the onset till the end of the Plateau (Fig. 2).

Then, we compared the duration of the entire CIE as well as that of the 'recovery' interval in to discuss completeness of sections and/or implications of different durations for regional paleoenvironmental responses (Section 4.2.2). The 'recovery' interval the duration of which we will compare does not correspond to the interval from the end of Plateau, i.e. when $\delta^{13}C$ starts decreasing till the end of the CIE, as mentioned in Fig. 2. To facilitate writing, we will hereafter take the 'recovery' phase as the interval from the CTB till the end of CIE. The end of CIE in the APB and Lower Saxony Basin was revised according to Poigny record, together with the proposed worldwide correlation (Fig. 2, Fig. 4, Fig. 5).

4.2.2. Duration of OAE2 and diachroneity of the Cenomanian-Turonian boundary

'Perturbation' interval at Poigny contains three and a half short eccentricity cycles (Fig. 2). At USGS#1 Portland core (WIB), the same interval includes five and a half short eccentricity cycles (Meyers et al., 2012a) (see Table 1 for the numbers of short eccentricity and precession cycles). Iona-1 and Angus cores (WIB), correlated to the USGS#1 Portland core to infer the position of CTB, also contain five and a half short eccentricity cycles in the 'perturbation' interval (Ma et al., 2014; Eldrett et al., 2015)

From the above comparison, Poigny core provides a significantly shorter duration than sections from the WIB. If the prominent ~3 m $\delta^{13}C$ oscillations at Poigny were orbitally paced by the short eccentricity cycle (Section 3, and argued below from other neighboring sections), a potential hiatus of two short eccentricity cycles could be inferred in the Poigny site.

A sharp lithological contact between the upper Cenomanian chalk and overlying Plenus Marl in the Paris Basin and surrounding areas was noted as an angular unconformity through basin-scale sedimentological correlations (Lasseur, 2007 and references therein). The same surface was interpreted as erosional surface in Eastbourne (UK) (Jefferies, 1962; Gale et al., 1993; Paul et al., 1999; Mortimore et al., 2001; Jarvis et al., 2006). Cyclostratigraphic interpretation from Poigny $\delta^{13}C$ data reveals low sedimentation rates at the onset of CIE (Fig. 2, Fig. 3), hence corroborating a possible sedimentary gap.

Although we point out a potential gap affecting the duration of OAE2, assessment of the duration of the whole CIE among the compared sections does not concur with the hypothesis of a significant gap. Indeed, the whole CIE contains approximately eight to eight and a half short eccentricity cycles in several sections (Fig. 4). At Poigny, the CIE is exceptionally well-defined, together with distinct onset and end, and includes eight and a small part of ninth short eccentricity cycles (Fig. 2). At Gongzha section, the whole CIE is also well-defined and covers nearly eight to eight and a half short eccentricity cycles. In the WIB, the end of CIE is not evident in USGS#1 Portland (Sageman et al., 2006), but could be placed from the Angus core, especially from Iona-1 core (Ma et al., 2014; Eldrett et al., 2015, Eldrett et al., 2017). The whole CIE in the WIB (Angus and Iona-1 cores) contains nearly eight to eight and a half short eccentricity cycles (Fig. 4).

The record of the same number of short eccentricity cycles within the CIE between world-wide correlated sections points to stratigraphic completeness of Poigny record, thus weakening the hypothesis of significant hiatus at the onset of CIE. Nevertheless, the impact of this presumed hiatus cannot be ruled out in depositional environments with lower sedimentation rates, resulting in condensed sections and major erosional surfaces (Jefferies, 1962; Gale et al., 1993; Hilbrecht and Dahmer, 1994; Voigt et al., 2008).

The close duration of the whole CIE, as inferred from different sections, also implies that 'perturbation' interval is shorter at Poigny, while 'recovery' interval is longer in WIB sections. In England, the Eastbourne section shows correlatable $\delta^{13}C$ record to Poigny, and in particular documents a shorter 'recovery' phase (Fig. 5). The Eastbourne section exhibits almost 17 and a half to 18 precession cycles within 'perturbation' interval (Fig. 5). Poigny core documents in 'perturbation' interval 18 and a half to 21 precession cycles (Fig. 3, Fig. 5). Interestingly, cyclostratigraphic analysis of the highly-resolved $\delta^{13}C$ data in the Eastbourne section, using two datasets of Paul et al. (1999) and Tsikos et al. (2004), points to 17 and a half to 18 and a half precession cycles within 'perturbation' interval (Fig. 6). This result is in accordance with field cyclostratigraphic interpretations (Fig. 5, Gale, 1995; Gale et al., 1993, Gale et al., 1999). Also, short eccentricity $\delta^{13}C$ related cycles AP1 through AP5 are highly resolved in the Eastbourne section (Fig. 6 and Supplementary Fig. S3).

In Germany, highly-resolved OAE2 cyclostratigraphy of the Wunstorf core (Lower Saxony Basin, Voigt et al., 2008) also provides a shorter 'perturbation' interval (Fig. 5). In particular, this interval contains nearly 18 to 21 precession cycles, close to those inferred from the APB. Despite the close number of precession cycles in the APB and Lower Saxony Basin, we should note that there is a discrepancy in the record of short eccentricity cycles within 'perturbation' interval. Poigny core and Eastbourne section document in average three and a half cycles, while Wunstorf core records four cycles. This discrepancy of a half short eccentricity cycle (or less) was highlighted between Wunstorf core and Eastbourne section (Voigt et al., 2008). We cannot relate such difference to an actual offset and/or to hiatus, given the record of almost the same number of precession cycles in the two basins on one hand, and especially the uncertainty intervals on the CTB that exist at Poigny and Wunstorf, on the other hand.

In Tunisia, pronounced cyclic lithologies in the Oued Bahloul Formation, which were likely paced by the precession and short eccentricity cycles, yield duration of ~335 kyr for 'perturbation' interval (Caron et al., 1999). This duration is closer to ~350 kyr duration from Europe (e.g., Eastbourne), than ~550 kyr from the WIB. The CTB in the Oued Bahloul Formation is precisely defined on the basis of ammonites (Caron et al., 1999, Caron et al., 2006; Amédro et al., 2005); thus, such formation potentially indicates that 'perturbation' interval is again shorter in North Africa than in WIB (Fig. 7).

Therefore, because the total duration of the CIE is almost the same from different sections and basins, and 'perturbation' interval is significantly shorter in the APB and Lower Saxony Basin but longer in the WIB (Table 1), we conclude that sedimentary gap at the onset of CIE would have a minor effect on the estimate of the total duration of CIE. The duration of this gap at Poigny, Eastbourne and Wunstorf sections could not be at the scale of short eccentricity cycle, as argued here by the cyclostratigraphic analyses and correlation (compare Fig. 2, Fig. 6B). Rather, it would be in the order of few tens of kyr, or at the scale of precession cycles.

Difference in durations of 'perturbation' and 'recovery' intervals between basins implies that the CTB is diachronous. Based on cyclostratigraphic approach, such diachroneity between the APB and WIB could be quantified at ~200 kyr (equivalent to two 100 kyr eccentricity cycles). Additional evidence for such biotic offset comes from calcareous nannofossil biostratigraphy, although preservation and/or different taxonomic concepts among researchers as well as reproducibility and reliability of biohorizons could induce apparent diachroneity (Section 2.1.2, see also Fig. 8A). The Base of *Q. gartneri*, which is one of the main biohorizons that marks the CTB (e.g.,

Tsikos et al., 2004), also recognized at Poigny record, hints at a significant offset between the APB and WIB. This biostratigraphic marker is situated within AP5 to mid-AP6 short eccentricity cycles in the APB, but at the end of AP7 to mid-AP8 cycles in the WIB (Fig. 4, Fig. 8). Although we cannot strictly quantify the timing offset of the Base of *Q. gartneri* between the two basins because of great uncertainties in its definition within sections and among researchers (Fig. 8), such result points to a younger *Q. gartneri* biohorizon in the WIB with respect to its equivalent in the APB. Thus, the temporally shifted *Q. gartneri* biohorizon again concurs with the hypothesis of diachroneity of the CTB, defined on the basis of ammonites. Also, the diachroneity of several key foraminiferal bio-events, which has been widely argued (Section 4.1), is further highlighted through cyclostratigraphic and $\delta^{13}C$ correlations that we propose (e.g., Fig. 4 and Supplementary Fig. S4). In particular, the Top of *W. archaeocretacea,* and Base of *H. helvetica* are temporally shifted between sedimentary basins and environments (Fig. 4, Fig. 5 and Supplementary Fig. S4). At Iona-1 and USGS♯1 Portland cores (WIB), they were recognized at around the end of CIE, at the end of short eccentricity cycle number 9. At Wunstorf (Lower Saxony Basin), they occurred at the end of cycle 6. At Eastbourne (APB), they were identified at the end of cycle 4 (Cycle AP4). Interestingly, these two key foraminiferal bio-events are temporally shifted to younger strata in the WIB with respect to their equivalents in the APB (Eastbourne). This again supports the idea of a younger CTB in the WIB against an older CTB in the APB.

We suggest that such significant temporal offset is not exclusively related to the definition of the stratigraphic position of CTB. The CTB in both basins (e.g., Eastbourne vs Pueblo reference sections) was precisely defined on the basis of ammonites. Diachroneity of CTB had been evoked among other options by Voigt et al. (2008) to explain the offset between Wunstorf core and Pueblo-Portland composite section in WIB. Based on rigorous cyclostratigraphic comparison between Wunstorf and Pueblo-Portland records, Voigt et al. (2008) assessed this diachroneity at 100 to 150 kyr.

A more detailed $\delta^{13}C$ correlation between sections from the APB and WIB, along with a revised location of $\delta^{13}C$ peaks indicates that the CTB is not situated in the same position on the CIE in the two basins. It is above peak C in APB and below it in WIB (Fig. 8B). Additionally, the Holywell Event is almost three short eccentricity cycles above the CTB in APB, but by only one short eccentricity cycle above it in WIB (see also Fig. 4), pointing again to the diachroneity of CTB between the two basins.

We hypothesize that diachroneity of the CTB is the consequence of shifted biotic responses between basins. This would reflect regional responses to the global OAE2 paleoenvironmental perturbation, which depend on characteristics of each ocean and sea. The most intriguing finding is that key calcareous nannofossil, foraminiferal and ammonite biohorizons are shifted towards younger strata in WIB with respect to APB. Such disturbed regional conditions would have direct influence on faunal turnovers, and thus, on the timing of appearances and disappearances of marine organisms. We conclude that the OAE2 extreme paleoenvironmental perturbation may have affected marine biotas of pelagic/planktonic communities, hence leading to inter-basinal diachroneity in the main biostratigraphic datums. Future studies should focus on the cause of an older CTB in WIB versus a younger CTB in Europe (Fig. 8). According to cyclostratigraphic approach and correlations, the entry of *W. devonense* was at least 200 kyr later in WIB than in Europe.

4.3. Volcanic amplification of eccentricity driven carbon cycle

The OAE2 interval is a key period, during which Earth experienced profound changes in the biogeochemical cycles as attested by severe changes in chemical, physical, paleontological and sedimentological characteristics of the sediment (see Jenkyns, 2010 for a review). The well-recorded feature of the OAE2 and other OAEs is the perturbation to the global carbon cycle, expressed by a pronounced (> 2‰) CIE in both marine and continental sedimentary environments.

The OAE2 exhibits pronounced short-term $\delta^{13}C$ variations, with three distinct, most important $\delta^{13}C$ peaks (e.g., Peaks A, B and C, Fig. 2) superimposed on the overall positive CIE (e.g., Paul et al., 1999; Jarvis et al., 2006, Jarvis et al., 2011; Erbacher et al., 2005; Voigt et al., 2008). Poigny $\delta^{13}C$ data document these three peaks with an additional peak we labelled as Peak Cp, which is stronger than Peak C (Fig. 2).

These $\delta^{13}C$ peaks are readily correlatable in the APB, and form the 'Plateau', characterized by elevated $\delta^{13}C$ values (Paul et al., 1999; Jarvis et al., 2006, Jarvis et al., 2011, and this study, Fig. 5). The stationary phase (or Plateau) is characterized by prominent, cyclic $\delta^{13}C$ oscillations with the peaks being extremes of the cycles.

While $\delta^{13}C$ peaks A and B could tentatively be correlated between different sections, correlation of peak C is more problematic (Fig. 8). For instance, in relatively highly-resolved $\delta^{13}C$ data at the Iona-1 core (WIB), peak C is placed in the decreasing part of CIE, i.e. after a $\delta^{13}C$ 'Plateau' of elevated $\delta^{13}C$ values (Eldrett et al., 2015 their Fig. 4). In the same basin at the Turonian GSSP Pueblo section, peak C is placed within the Plateau (e.g., Bowman and Bralower, 2005). This again points to the difficulty in correlating peak C even within the same basin. In the Gongzha section (southern Tibet, China), which is likely the most expanded known OAE2 section, the CIE is recorded with high fidelity (Li et al., 2017). Multiple $\delta^{13}C$ cyclic oscillations within the CIE could clearly be observed from this section, matching very likely the short eccentricity band. Distinction of the three peaks A, B, and C (esp. A and B) from this section is not readable. Although the study of Li et al. (2017) focused more on orbitally paced magnetic susceptibility variations, their highly-resolved $\delta^{13}C$ data support the idea of short eccentricity control of the carbon cycle within the OAE2.

These prominent short-term $\delta^{13}C$ variations within the CIE have been intensively studied in terms of pulses in CO_2 from volcanism, especially for the two main peaks A and B (e.g., Kuroda et al., 2007; Forster et al., 2007; Turgeon and Creaser, 2008; Du Vivier et al., 2014, Du Vivier et al., 2015). Time-series analysis of highly-resolved $\delta^{13}C$ data of Poigny indicates that peaks A and B match extremes in short eccentricity cycling. Additionally, Poigny record indicates that all important, internal short-term $\delta^{13}C$ oscillations within the CIE, which have been widely studied (e.g., Jarvis et al., 2006; Voigt et al., 2008), match the short eccentricity cycle band.

Previous studies showed that volcanically released CO_2 is the important agent for the OAE2 carbon cycle perturbation (Jenkyns, 2010 and references therein). Thus, we hypothesize that excessively released greenhouse gases from volcanic Large Igneous Provinces. This does not mean that short eccentricity drove volcanic activity. Instead, volcanically released greenhouse gases may have been amplifying factors, which may have enhanced the expression (or record) in the sediment of the carbon cycle, forced by precession and eccentricity. Thus, atmospheric greenhouse gases from volcanism may have played a major role in the amplification and expression of the orbitally paced carbon cycle in the sedimentary record. Previous studies have shown exceptional record of the carbon cycle during early Cenozoic extreme greenhouse warmth (e.g., Boulila et al., 2012).

5. Conclusions

High-resolution (~2 kyr) bulk carbonate $\delta^{13}C$ data of Poigny drill-core in the Paris Basin detects with high fidelity positive CIE associated to OAE2. The CIE at Poigny is correlatable to its equivalents in several previously studied sections, and is recorded with the same amplitude (~2.5‰) than its lateral equivalent in the APB in Eastbourne (UK) section. Time-series analysis of Poigny $\delta^{13}C$ record reveals Earth's orbital parameters (precession, obliquity and short eccentricity) with the short eccentricity signal being the most prominent.

Astronomical calibration of the CIE based on short eccentricity yields a duration, equivalent to eight and more likely eight and a half short eccentricity cycles (~850 kyr).

Cyclostratigraphic results and correlation with previous key records of the OAE2, together with a newly revised definition of the stratigraphic extent of CIE, indicate a close duration of the whole CIE in the APB, Lower Saxony Basin and WIB, and northern margin of Indian plate. However, duration of the interval from the onset of CIE to the Cenomanian-Turonian boundary (CTB) in WIB, APB, and Lower Saxony Basin where the CTB is well-defined by ammonites is considerably different. This interval contains five and a half short (100 kyr) eccentricity cycles in the WIB (equivalent to a duration of ~550 kyr), and only three and a half short (100 kyr) eccentricity cycles in the APB and Lower Saxony Basin (equivalent to a duration of ~350 kyr). Assuming that the onset of CIE is synchronous between basins, such cyclostratigraphic correlation suggests a ~200 kyr younger CTB in the WIB than in Europe.

Correlation of short eccentricity-scale $\delta^{13}C$ variations at Poigny with previous characterization of the CIE indicates that the main, distinct and well-known $\delta^{13}C$ peaks (e.g., Peaks A, B and C), as well as other characteristics of small-scale $\delta^{13}C$ excursions (e.g., Holywell Event) correspond to extremes in short eccentricity cycling. Previous studies suggested a potential link between overall CIE and volcanism. Accordingly, we infer that excessively released greenhouse gases from volcanic eruptions associated with large igneous provinces may have amplified the response of the orbitally paced carbon cycle.

Acknowledgments

We acknowledge Damien Gendry at Rennes 1 University for his significant help to access to the Poigny drill-core. During her master degree J.B. (supervised by S.B., B.G. and L.L) was financially supported by ANR-Labex Matisse and ISTeP laboratory. S.B., G.C. and B.G. were supported by French ANR Project AstroMeso. We thank very much anonymous reviewers for their very helpful reviews.

References

F. Amédro, H. Accarie, F. Robaszynski - Position de la limite Cénomanien-Turonien dans la formation Bahloul de Tunisie centrale: apports intégrés des ammonites et des isotopes du carbone (δ13C). Eclogae Geol. Helv., 98 (2005), pp. 151-167

I.R. Barker, D.E. Moser, S.L. Kamo, A.G. Plint - High-precision U-Pb zircon ID-TIMS dating of two regionally-extensive bentonites: Cenomanian stage, Western Canada Foreland Basin, Can. J. Earth Sci., 48 (2011), pp. 543-556

B. Bomou, T. Adatte, A.A. Tantawy, H. Mort, D. Fleitmann, Y. Huang, K.B. Föllmi - The expression of the Cenomanian-Turonian oceanic anoxic event in Tibet. Palaeogeogr. Palaeoclimatol. Palaeoecol., 369 (2013), pp. 466-481

S. Boulila, L.A. Hinnov - A review of tempo and scale of the early Jurassic Toarcian OAE: implications for carbon cycle and sea level variations. Newsl. Stratigr. (2017), 10.1127/nos/2017/0374

S. Boulila, B. Galbrun, J. Laskar, H. Pälike - A ~9 Myr cycle in Cenozoic ^{13}C record and long-term orbital eccentricity modulation. Is there a link? Earth Planet. Sci. Lett., 317–318 (2012), pp. 273-281

A.R. Bowman, T.J. Bralower - Paleoceanographic significance of high-resolution carbon isotope records across the Cenomanian-Turonian boundary in the Western Interior and New Jersey coastal plain, USA. Mar. Geol., 217 (2005), pp. 305-321

T.J. Bralower, J.A. Bergen - Cenomanian-Santonian calcareous nannofossil biostratigraphy of a transect of cores drilled across the western interior seaway. W.E. Dean, M.A. Arthur (Eds.), Stratigraphy and Paleoenvironments of the Cretaceous Western Interior Seaway, U.S.A: SEPM. Concepts in Sedimentology and Paleontology, 6 (1998), pp. 59-77

M. Caron, F. Robaszynski, F. Amédro, F. Baudin, J.-F. Deconinck, P. Hochuli, K. Von Salis-Perch Nielsen, N. Tribovillard - Estimation de la durée de l'événement anoxique global au passage Cénomanien Turonien. Approche cyclostratigraphique dans la Formation Bahloul en Tunisie centrale. Bulletin de la Société géologique de France, 170 (1999), pp. 145-160

M. Caron, S. Dall'Agnolo, H. Accarie, E. Barrera, E.G. Kauffman, F. Amédro, F. Robaszynski - High-resolution stratigraphy of the Cenomanian-Turonian boundary interval at Pueblo (USA) and Wadi Bahloul (Tunisia): stable isotope and bio-events correlation. Gebios, 39 (2006), pp. 171-200

G. Charbonnier, S. Boulila, J.E. Spangenberg, T. Adatte, K.B. Föllmi, J. Laskar - Obliquity pacing of the hydrological cycle during the Oceanic Anoxic Event 2 ; Earth Planet. Sci. Lett., 499 (2018), pp. 266-277

W.S. Cleveland - Robust locally weighted regression and smoothing scatterplots. J. Am. Stat. Assoc., 74 (1979), pp. 829-836

W.A. Cobban, G.R. Scott - Stratigraphy and ammonite fauna of the Graneros Shale and Greenhorn Limestone near Pueblo, Colorado. United States Geological Survey, Professional Paper, 645 (1972), p. 108

M.J. Corbett, D.K. Watkins, J.J. Popspichal - A quantitative analysis of calcareous nannofossil bioevents of the late cretaceous (late Cenomanian-Coniacian) Western Interior Seaway and their reliability in established zonation schemes. Mar. Micropaleontol., 109 (2014), pp. 30-45

D. Desmares, D. Grosheny, B. Beaudoin, S. Gardin, F. Gauthier-Lafaye - High resolution stratigrapic record constrained by volcanic ash beds at the Cenomanian-Turonian boundary in the Western Interior Basin, USA. Creatceous Res., 28 (2007), pp. 561-582

A.D.C. Du Vivier, D. Selby, B.B. Sageman, I. Jarvis, D.R. Gröcke, S. Voigt - Marine $^{187}Os/^{188}Os$ isotope stratigraphy reveals the interaction of volcanism and ocean circulation during Oceanic Anoxic Event 2. Earth Planet. Sci. Lett., 389 (2014), pp. 23-33

A.D.C. Du Vivier, A.D. Jacobson, G.O. Lehn, D. Selby, M.T. Hurtgen, B.B. Sageman - Ca isotope stratigraphy across the Cenomanian-Turonian OAE2: links between volcanism, seawater geochemistry, and the carbonate fractionation factor. Earth Planet. Sci. Lett., 416 (2015), pp. 121-131

J.S. Eldrett, C. Ma, S.C. Bergman, B. Lutz, F.J. Gregory, P. Dodsworth, M. Phipps, P. Hardas, D. Minisini, A. Ozkan, J. Ramezani, S.A. Bowring, S.L. Kamo, K. Ferguson, C. Macaulay, A.E. Kelly - An astronomically calibrated stratigraphy of the Cenomanian, Turonian and earliest Coniacian from the cretaceous Western Interior Seaway, USA: Implications for global chronostratigraphy ; Cretac. Res., 56 (2015), pp. 316-344

J.S. Eldrett, P. Dodsworth, C. Bergman, M. Wright, D. Minisini - Water-mass evolution in the cretaceous Western Interior seaway of North America and equatorial Atlantic. Clim. Past, 13 (2017), pp. 855-878

M. Elrick, R. Molina-Garza, R. Duncan, L. Snow - C-isotope stratigraphy and palaeoenvironmental changes across OAE2 (mid-cretaceous) from shallow-water platform carbonates of southern Mexico. Earth Planet. Sci. Lett., 277 (2009), pp. 295-306

J. Erbacher, O. Friedrich, P. Wilson, H. Birch, J. Mutterlose - Stable organic carbon isotope stratigraphy across Oceanix Anoxic Event 2 of Demerara rise, western tropical Atlantic. Geochem. Geophys. Geosyst., 6 (2005), pp. 1-9

F. Falzoni, M.R. Petrizzo, M. Caron, R.M. Leckie, K. Elderbak - Age and synchronicity of planktonic foraminiferal bioevents across the Cenomanian–Turonian boundary interval (late cretaceous). Newsl. Stratigr. (2018), 10.1127/nos/2018/0416

A.G.S. Fernando, R. Takashima, H. Nishi, F. Giraud, H. Okada - Calcareous nannofossil biostratigraphy of the Thomel Level (OAE2) in the Lambruisse section, Vocotian Basin, Southeast France. Geobios, 43 (2010), pp. 45-57

A. Forster, S. Schouten, K. Moriya, P.A. Wilson, J.S. Sinninghe Damsté - Tropical warming and intermittent cooling during the Cenomanian/Turonian oceanic anoxic event 2: sea surface temperature records from the equatorial Atlantic. Paleoceanography, 22 (2007), 10.1029/2006PA001349 PA1219

A.S. Gale - Cyclostratigraphy and correlation of the Cenomanian stage in Western Europe. M.R. House, A.S. Gale (Eds.), Orbital Forcing Timescales and Cyclostratigraphy, 85, Geological Society, London, Special Publication (1995), pp. 177-197

A.S. Gale, W.K. Christensen - Occurrence of the belemnite *Actinocamax plenus* in the Cenomanian of SE France and its significance. Bull. Geol. Soc. Den., 43 (1996), pp. 68-77

A.S. Gale, H.C. Jenkyns, W.J. Kennedy, R.M. Corfield - Chemostratigraphy versus biostratigraphy: data from around the Cenomanian–Turonian boundary. J. Geol. Soc. Lond., 150 (1993), pp. 29-32

A.S. Gale, J.R. Young, N.J. Shackleton, S. Crowhurst, D.S. Wray - Orbital tuning of Cenomanian marly chalk successions; towards a Milankovitch time scale for the late cretaceous. Philosoph. Trans. Royal Soc. Series A, 357 (1999), pp. 1815-1829

A.S. Gale, W.J. Kennedy, S. Voigt, I. Walaszczyk - Stratigraphy of the Upper Cenomanian-lower Turonian Chalk succession at Eastbourne, Sussex, UK: ammonites, inoceramid, bivalves and stables carbon isotopes. Cretac. Res., 26 (2005), pp. 460-487

A.S. Gale, H.C. Jenkyns, H. Tsikos, Y. van Breugel, J.S. Sinninghe Damsté, C. Bottini, E. Erba, F. Russo, F. Falzoni, M.R. Petrizzo, A.J. Dickson, D.S. Wray - High-resolution bio- and chemostratigraphy of an expanded record of Oceanic Anoxic Event 2 (late Cenomanian-early Turonian) at Clot Chevalier, near Barrême, SE France (Vocontian Basin, SE France). Newsl. Stratigr. (2018), 10.1127/nos/2018/0445

B.U. Haq, J. Hardenbol, P.R. Vail - The new chronostratigraphic basis of Cenozoic and Mesozoic sea-level cycles. C.A. Ross, D. Haman (Eds.), Timing and Depositional History Of Eustatic Sequences Constraints On Seismic stratigraphy: Cushman Foundation for Foraminiferal Research, 24, Special Publications (1987), pp. 7-13

P. Hardas, J. Mutterlose - Calcareous nannofossil biostratigraphy of the Cenomanian/ Turonian boundary interval of ODP Leg 207 at the Demerara rise. Rev. Micropaleontol., 49 (2006), pp. 165-179

H. Hilbrecht, D.D. Dahmer - Sediment dynamics during the Cenomanian-Turonian (cretaceous) Oceanic Anoxic Event in northwestern Germany. Facies, 30 (1994), pp. 63-84

B.T. Huber, R. Norris, K.G. MacLeod - Deep-sea paleotemperature record of extreme warmth during the cretaceous. Geology, 30 (2002), pp. 123-126

M.C. Janin - Corrélation des forages Craie 700 d'après les nannofossiles calcaires. Bull. Inf. Géol. Bassin Paris, 37 (2) (2000), pp. 52-58

I. Jarvis, A.S. Gale, H.C. Jenkyns, M.A. Pearce - Secular variation in late cretaceous carbon isotopes: a new $\delta^{13}C$ carbonate reference curve for the Cenomanian–Campanian (99.6–70.6 Ma). Geol. Mag., 143 (2006), pp. 561-608

I. Jarvis, J.S. Lignum, D.R. Gröcke, H.C. Jenkyns, M.A. Pearce - Black shale deposition, atmospheric CO2 drawdown, and cooling during the Cenomanian-Turonian Oceanic Anoxic Event. Paleoceanography, 26 (2011) PA3201

R.P.S. Jefferies - The palaeoecology of the Actinocamax plenus subzone (lowest Turonian) in the Anglo-Paris Basin. Palaeontology, 4 (1962), pp. 609-647

H.C. Jenkyns - Geochemistry of oceanic anoxic events. Geochem. Geophys. Geosyst., 11 (2010), 10.1029/2009GC002788 Q03004

Y.J. Joo, B.B. Sageman - Cenomanian to Campanian carbon isotope chemostratigraphy from the Western Interior Basin. USA. J. Sediment. Res., 84 (2014), pp. 529-542

G. Keller, A. Pardo - Paleoecology of the Cenomanian –Turonian Stratotype Section (GSSP) at Pueblo, Colorado. Mar. Micropleontol., 51 (2004), pp. 95-128

G. Keller, Q. Han, T. Adatte, S. Burns - Paleoenvironment of the Cenomanian–Turonian transition at Eastbourne, England. Cretac. Res., 22 (2001), pp. 391-422

G. Keller, Z. Berner, T. Adatte, D. Stueben - Cenomanian-Turonian $\delta^{13}C$ and $\delta^{18}O$, sea level and salinity variations at Pueblo, Colorado. Palaeogeogr. Palaeoclimatol. Palaeoecol., 211 (2004), pp. 19-43

W.J. Kennedy, W.A. Cobban - Stratigraphy and interregional correlation of the CenomanianeTuronian transition in the Western Interior of the United States near Pueblo, Colorado, a potential boundary stratotype for the base of the Turonian Stage. Newsl. Stratigr., 24 (1991), pp. 1-33

W.J. Kennedy, I. Walaszczyk, W.A. Cobban - Pueblo, Colorado, U.S.A., candidate Global Boundary Stratotype Section and Point for the base of the Turonian Stage of the Cretaceous, and for the base of the Middle Turonian Substage, with a revision of the Inoceramidae. Acta Geol. Pol., 50 (2000), pp. 295-334

W.J. Kennedy, I. Walaszczyk, W.A. Cobban - The global boundary stratotype section and point for the base of the Turonian stage of the cretaceous: Pueblo, Colorado, U.S.A. Episodes, 28 (2005), pp. 93-104

J. Kuroda, N.O. Ogawa, M. Tanimizu, M.F. Coffin, H. Tokuyama, H. Kitazato, N. Ohkouchi - Contemporaneous massive subaerial volcanism and late cretaceous Oceanic Anoxic Event 2. Earth Planet. Sci. Lett., 256 (2007), pp. 211-223

J. Laskar, P. Robutel, F. Joutel, M. Gastineau, A.C.M. Correia, B. Levrard - A long-term numerical solution for the insolution quantities of the Earth. Astron. Astrophys., 428 (2004), pp. 261-285

E. Lasseur - La Craie du Bassin de Paris (Cénomanien-Campanien, Crétacé supérieur). Sédimentologie de faciès, stratigraphie séquentielle et géométrie 3D. PhD Thesis. Rennes 1 University, France (2007), p. 436

X.H. Li, H.C. Jenkyns, C.S. Wang, X.M. Hu, X. Chen, Y.S. Wei, Y.J. Huang, J. Cui - Upper cretaceous carbon and oxygen isotope stratigraphy of hemipelagic carbonate facies from southern Tibet, China. J. Geol. Soc. Lond., 163 (2006), pp. 375-382

Y.X. Li, I.P. Montañez, Z. Liu, L. Ma - Astronomical contraints on global carbon-cycle perturbation during Oceanic Anoxic Event 2 (OAE2). Earth Planet. Sci. Lett., 462 (2017), pp. 35-46

C. Linnert, J. Mutterlose, J. Erbacher - Calcareous nannofossils of the Cenomanian/Turonian boundary interval from the Boreal Realm (Wunstorf, Northwest Germany). Mar. Micropaleontol., 74 (2010), pp. 38-58

C. Linnert, J. Mutterlose, R. Mortimore - Calcareous nannofossils from Eastbourne (Southeastern England) and the paleoceanography of the Cenomanian–Turonian boundary interval. Palaios, 26 (2011), pp. 298-313

C. Ma, S.R. Meyers, B.B. Sageman, B.S. Singer, B.R. Jicha - Testing the astronomical time scale for oceanic anoxic event 2, and its extension into Cenomanian strata of the Western Interior Basin (USA). Geol. Soc. Am. Bull. (2014), 10.1130/b30922.1

M.E. Mann, J.M. Lees - Robust estimation of background noise and signal detection in climatic time series. Clim. Chang., 33 (1996), pp. 409-445

C. Mégnien, F. Hanot - Deux forages scientifiques profonds pour étudier les phénomènes diagénétiques de grande ampleur dans la craie du bassin de Paris. Bull. Inf. Géol. Bassin Paris, 37 (2000), pp. 3-7
S.R. Meyers - Astrochon: An R Package for Astrochronology, (2014), (Available at cran.rproject. org/web/packages/astrochron/index.html)
S.R. Meyers, B.B. Sageman, M.A. Arthur - Obliquity forcing of organic matter accumulation during Oceanic Anoxic Event 2. Paleoceanography (2012), pp. 1-19
S.R. Meyers, S. Siewert, B. Singer, B. Sageman, D. Condon, J. Obradovich, B. Jicha, D. Sawyer - Intercalibration of radioisotopic and astrochronologic time scales for the Cenomanian-Turonian boundary interval, Western Interior Basin, USA. Geology, 40 (2012), pp. 7-10
R.N. Mortimore, C.J. Wood, R.W. Gallois - British upper cretaceous stratigraphy. Geol. Conserv. Rev. Series, 23 (2001) (558p)
D. Paillard, L. Labeyrie, P. Yiou - Macintosch program performs timeseries analysis. Eos, 77 (1996), p. 379
C.R.C. Paul, M.A. Lamolda, S.F. Mitchell, M.R. Vaziri, A. Gorostidi, J.D. Marshall - The Cenomanian-Turonian boundary at Eastbourne (Sussex, UK): a proposed European reference section. Palaeogeogr. Palaeoclimatol. Palaeoecol., 150 (1999), pp. 83-121
S.W. Poulton, S. Henkel, C. März, H. Urquhart, S. Flögel, S. Kasten, J.S. Sinninghe Damsté, T. Wagner - A continental-weathering control on orbitally driven redox-nutrient cycling during cretaceous Oceanic Anoxic Event 2. Geology (11) (2015), pp. 963-966
L.M. Pratt, L.M. Pratt - Isotopic Studies of organic matter and carbonates in rocks of the Greenhorn Marine Cycle. E.G. Kauffman, F.B. Zelt (Eds.), Fine-GrainedDeposits Of Cyclic Sedimentary Processes, SEPM Field Trip Guidebook (1985), pp. 38-48
L.M. Pratt, C.N. Threlkeld - Stratigraphic significance of $^{13}C/^{12}C$ ratios in mid-cretaceous rocks of the Western Interior, U.S.A. D.F. Stott, D.J. Glass (Eds.), The Mesozoic of Middle North America. Canadian Society of Petroleum Geologists, 9 (1984), pp. 305-312
F. Robaszynski - Le forage de Poigny: description lithologique. Bull. Inf. Géol. Bassin Paris, 37 (2000), pp. 18-26
F. Robaszynski, J.P. Bellier - Biostratigraphie du Crétacé avec les foraminifères dans les forages de Poigny et de Sainte-Colombe. Bull. Inf. Géol. Bassin Paris, 37 (2000), pp. 59-65
F. Robaszynski, F. Amédro, M. Caron - La limite Cénomanien-Turonien et la Formation Bahloul dans quelques localités de Tunisie centrale. Cretac. Res., 14 (1993), pp. 477-486
F. Robaszynski, B. Pomerol, E. Masure, J.P. Bellier, J.F. Deconinck - Stratigraphy and stage boundaries in reference sections of the Upper cretaceous Chalk in the east of the Paris Basin; the 'Craie 700' Provins boreholes. Cretac. Res., 26 (2005), pp. 157-169
B.B. Sageman, J. Rich, M.A. Arthur, G.E. Birchfield, W.E. Dean - Evidence for Milankovitch periodicities in Cenomanian-Turonian lithologic and geochemical cycles, Western Interior U. S. J. Sediment. Res., 67 (1997), pp. 286-301
B.B. Sageman, S.R. Meyers, M.A. Arthur - Orbital time scale and new C-isotope record for Cenomanian-Turonian boundary stratotype. Geology, 34 (2006), pp. 125-128
A. Savitzky, M.J.E. Golay - Smoothing and differentiation of data by simplified least squares procedures. Anal. Chem. (8) (1964), pp. 1627-1639
S.O. Schlanger, H.C. Jenkyns - Cretaceous oceanic anoxic events: causes and consequences. Geol. Mijnb., 55 (1976), pp. 179-184
P.A. Scholle, M.A. Arthur - Carbon isotope fluctuations in cretaceous pelagic limestones: potential stratigraphic and petroleum exploration tool. Am. Assoc. Pet. Geol. Bull., 64 (1980), pp. 67-87
D.J. Thomson - Spectrum estimation and harmonic analysis. IEEE Proc., 70 (1982), pp. 1055-1096
H. Tsikos, H.C. Jenkyns, B. Walsworth-Bell, M.R. Petrizzo, A. Forster, S. Kolonic, E. Erba, I. Premoli-Silva, M. Baas, T. Wagner, J.S. Sinninghe Damsté - Carbon-isotope

stratigraphy by the Cenomanian-Turonian Oceanic Anoxic Event: correlation and implications based on three key localities. J. Geol. Soc. Lond., 161 (2004), pp. 711-719
S.C. Turgeon, R.A. Creaser - Cretaceous oceanic anoxic event 2 triggered by a massive magmatic episode. Nature, 454 (2008), pp. 323-326
S. Voigt, A.S. Gale, S. Flögel - Midlatitude shelf seas in the Cenomanian-Turonian greenhouse world: Temperature evolution and North Atlantic circulation. Paleoceanography, 19 (2004), 10.1029/2004PA001015 PA4020
S. Voigt, J. Erbacher, J. Mutterlose, W. Weiss, T. Westerhold, F. Wiese, M. Wilmsen, T. Wonik - The Cenomanian–Turonian of the Wunstorf section (North Germany): global stratigraphic reference section and new orbital time scale for oceanic anoxic event 2. Newsl. Stratigr., 43 (2008), pp. 65-89

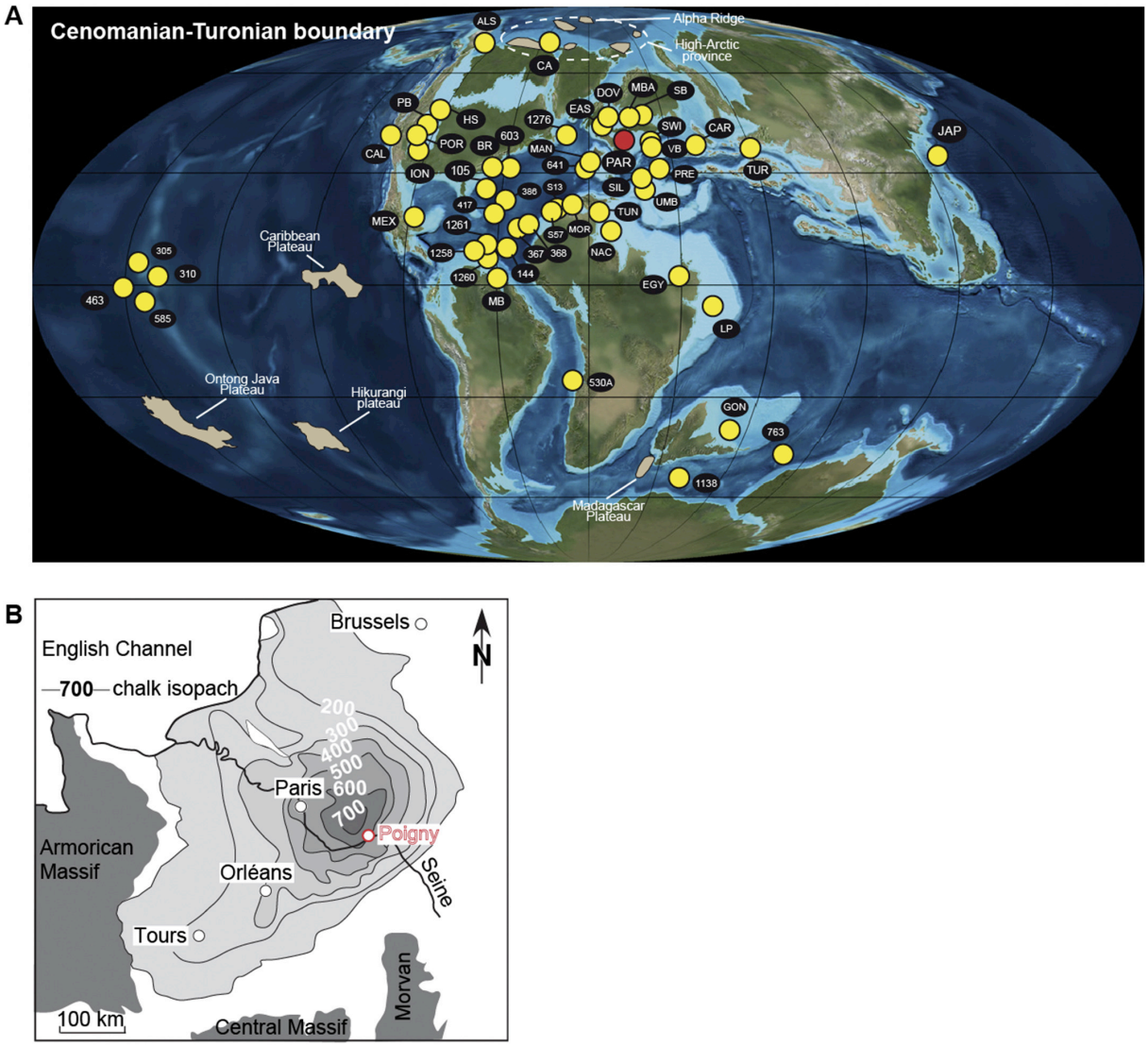

Fig. 1. (**A**) Previous OAE2 studied sites (yellow circles) including the presently studied Paris Basin site (red circle). Abbreviations: PAR: Paris Basin, GON: Gongzha, LP: Levant Platform, EGY: Egypt, JAP: Japan, TUR: Turkey, UMB: Umbria Marche Basin, NAC: North African Continental margin, MOR: Morocco, TUN: Tunisia, SIL: Sicily, VB: Vocontian Basin, CAR: Carpathians, SWI: Switzerland, MBA: Münsterland Basin, SB: Saxony Basin, DOV: Dover, EAS: Eastbourne, CA: Canadian Arctic, ALS: Alaska, PB: Pueblo, HS: Hot Springs, POR: Portland core, ION: Iona core, CAL: California, MEX: Mexico, MB: Maracaibo Basin. **(B)** Location of the studied Poigny 701 drill-core in a chalk isopach map of the Paris Basin (after Robaszynski et al., 2005). (For interpretation of the references to colour in this figure legend, the reader is referred to the web version of this article.)

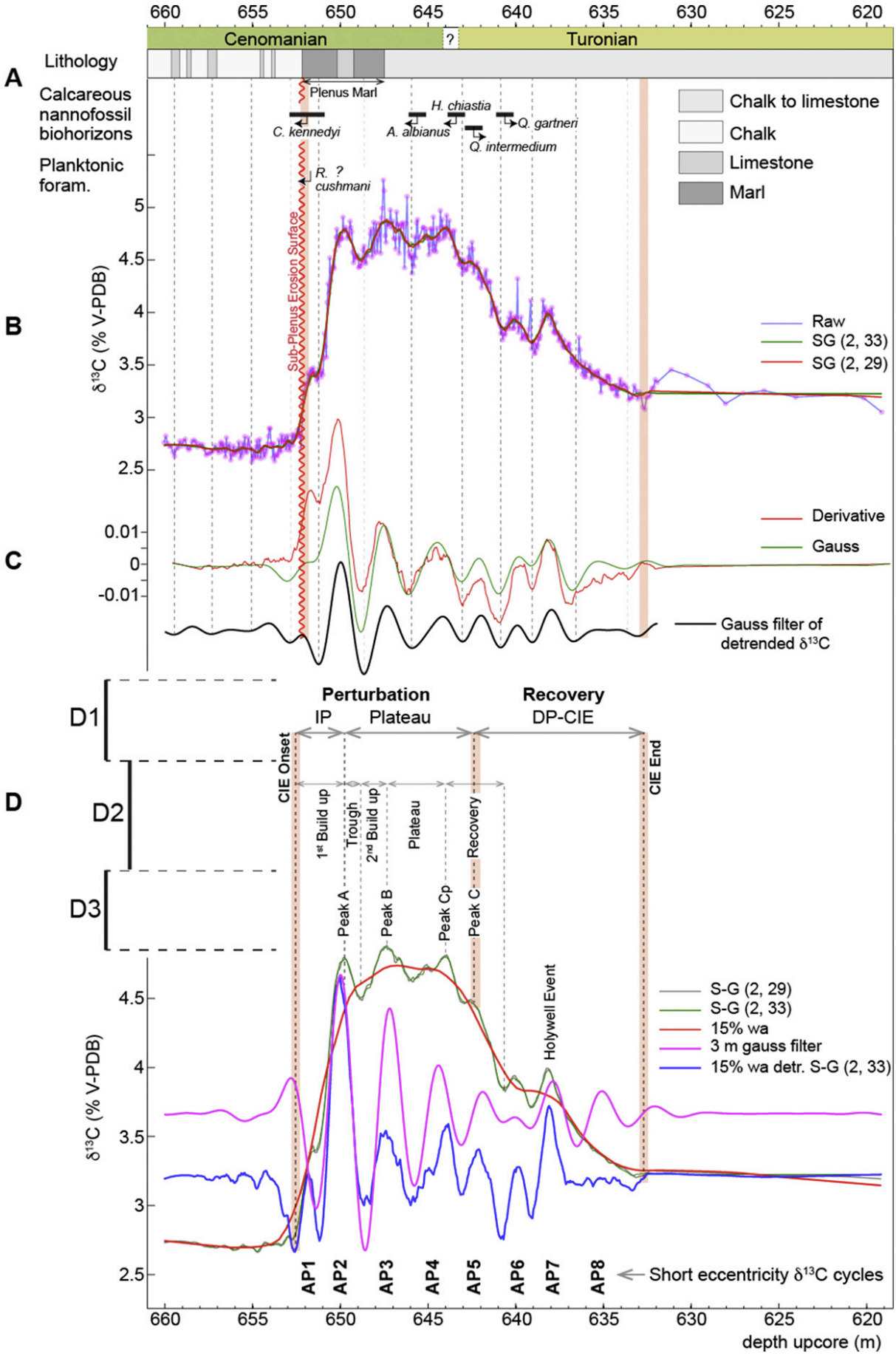
660
655
650
645
640
635
630
625
620
Cenomanian
?
Turonian
A
Lithology
Calcareous nannofossil biohorizons
Planktonic foram.
Plenus Marl
C. kennedyi
H. chiastia
A. albianus
Q. gartneri
Q. intermedium
R. ? cushmani
Sub-Plenus Erosion Surface
Chalk to limestone
Chalk
Limestone
Marl
B
δ13C (% V-PDB)
Raw
SG (2, 33)
SG (2, 29)
C
Derivative
Gauss
Gauss filter of detrended δ13C
D
D1
D2
D3
Perturbation
IP
Plateau
Recovery
DP-CIE
CIE Onset
CIE End
1st Build up
Trough
2nd Build up
Plateau
Recovery
Peak A
Peak B
Peak Cp
Peak C
Holywell Event
S-G (2, 29)
S-G (2, 33)
15% wa
3 m gauss filter
15% wa detr. S-G (2, 33)
AP1
AP2
AP3
AP4
AP5
AP6
AP7
AP8
Short eccentricity δ13C cycles
depth upcore (m)

Fig. 2. Integrated bio-lithostratigraphy and high-resolution stable carbon isotopes ($\delta^{13}C$) along with smoothing and filtering of $\delta^{13}C$ data of the OAE2 interval in the Paris Basin Chalk (Poigny Craie 701 drill-core). **(A)** Lithology and calcareous nannofossil data are from the present study, HO of the planktonic foraminifera *Rotalipora cushmani* (at 651.80 m from Robaszynski et al., 2005), is poorly constrained because of the difficulty in identifying species in the core below the Turonian-Coniacian boundary in relation with a poor preservation/sediment compaction as reported by Robaszynski and Bellier (2000). Possible position of CTB based on correlation with Eastbourne section (Fig. 5) is indicated. **(B)** Bulk cabonate $\delta^{13}C$ data along with S-G smoothing (with 2nd order polynomial, and 29 and 33 points) performed to highlight ~3 m oscillations superimposed on the CIE (see 'D'). **(C)** Isolation of the ~3 m cycles using S-G smoothing (with 2nd order polynomial, and a first-order derivative to eliminate the CIE) and the applied Gaussian bandpass (0.34 ± 0.2 cycles/m) filter to the smoothed curve; black curve is a Gaussian bandpass (0.34 ± 0.2 cycles/m) filtering of the 20% detrended weighted average of $\delta^{13}C$ data. **(D)** Characterization of the positive CIE associated to the OAE2, according to the present study (D1), Paul et al. (1999) (D2) and Jarvis et al., 2006, Jarvis et al., 2011 (D3). S-G and weighted average filters were applied to highlight $\delta^{13}C$ trends and oscillations. Because the short-term $\delta^{13}C$ oscillations within the CIE were most likely orbitally (short eccentricity) paced, we propose another definition of the CIE with respect to previous studies (e.g., Paul et al., 1999). The two main differences and input of Poigny $\delta^{13}C$ record with respect to previous studies are (i) the stratigraphic extent of CIE (more extended in this study), and (ii) the major peaks and internal excursions within the CIE, such as Peaks A, B, C and Holywell Event, correspond to extremes in short eccentricity cycling. Accordingly, we have labelled these $\delta^{13}C$ oscillations 'AP1' through 'AP8' for potential future correlation with highly resolved $\delta^{13}C$ data (Abbreviation AP: Anglo-Paris). Note that 'AP1' is most likely shortened by the hiatus. 'Cp' is an additional peak within the Plateau (Section 4.3). Orange bars represent limits of the two main phases of CIE: 'perturbation' and 'recovery' phases. Abbreviations IP and DP-CIE for increasing and decreasing parts of CIE.

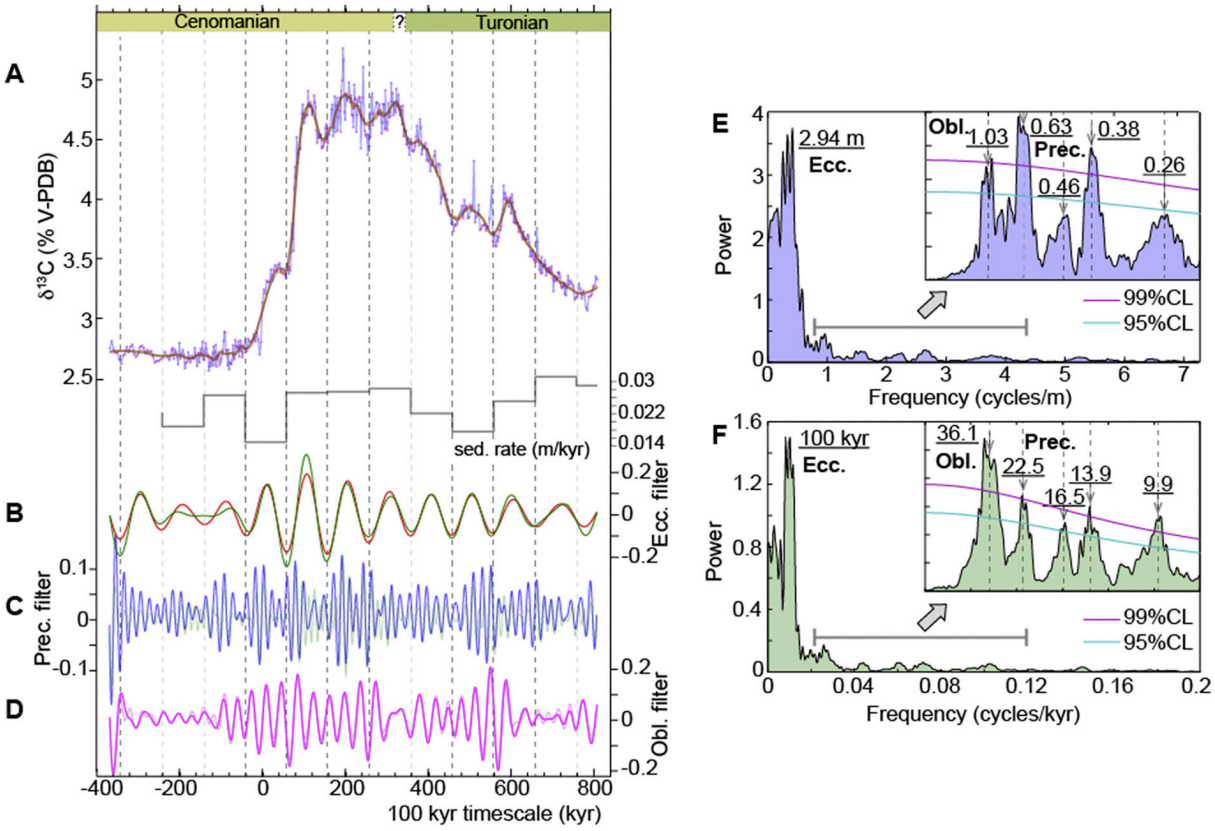

Fig. 3. Time-series analysis of $\delta^{13}C$ data and astronomical calibration of the OAE2 in the Paris Basin (Craie 701 drill-core). **(A)** 100 kyr short eccentricity tuned $\delta^{13}C$ data, along with S-G smoothing (Poly2, 29 and 33 points). The sedimentation rate is inferred from the 100 kyr tuning. **(B)** Gaussian bandpass filtering of the short eccentricity cycles (0.01 ± 0.002 cycles/kyr in blue and 0.01 ± 0.0035 cycles/kyr in green). **(C)** Gaussian bandpass filtering of the precession cycles (0.05 ± 0.01 cycles/kyr in blue and 0.06 ± 0.02 cycles/kyr in green). **(D)** Gaussian bandpass filtering of the obliquity cycles (0.027 ± 0.008 cycles/kyr in dark pink and 0.03 ± 0.01 cycles/kyr in light pink). **(E)** 2π-MTM power spectrum of the 20% weighted average of the $\delta^{13}C$ data in depth domain (OAE2 interval). *Inset*: Spectrum of S-G detrended data (Poly2, 29 points) applied to eliminate the CIE and short eccentricity band. **(F)** 2π-MTM power spectrum of the 20% weighted average of the $\delta^{13}C$ data in time domain. *Inset*: Spectrum of S-G detrended data (Poly2, 29 points) applied to eliminate the CIE and short eccentricity band. Abbreviations: 'Ecc.' for short eccentricity, 'Obl.' for obliquity and 'Prec.' for precession. (For interpretation of the references to colour in this figure legend, the reader is referred to the web version of this article.)

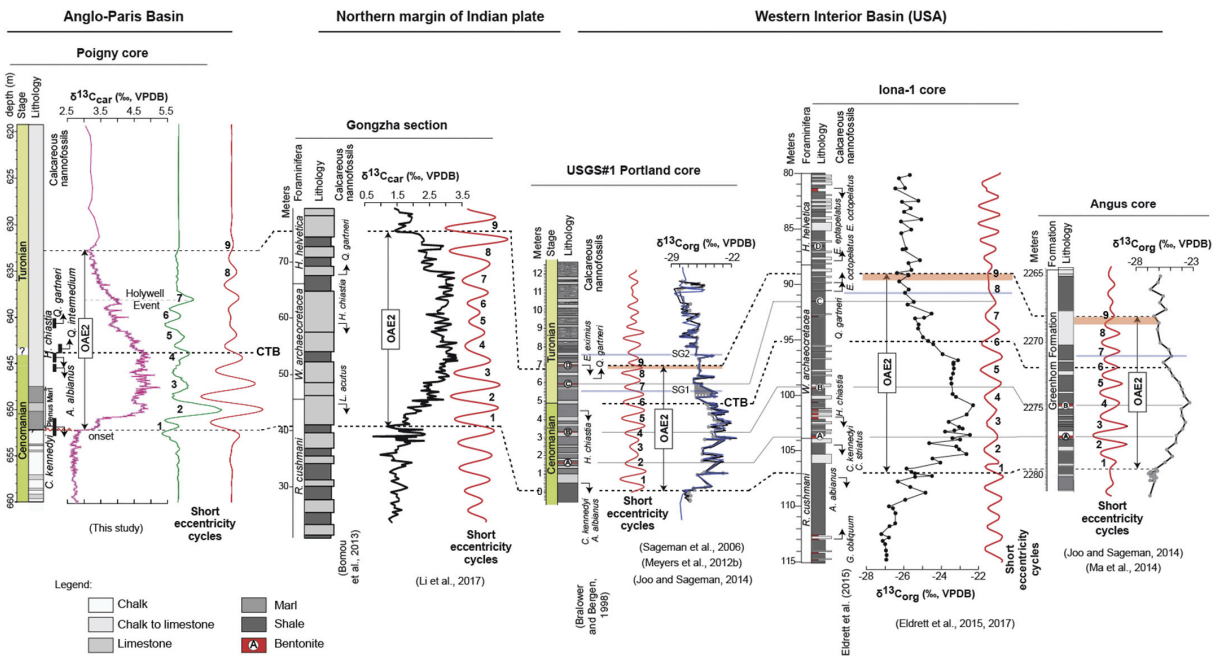

Fig. 4. Carbon-isotope and cyclostratigraphic correlation between OAE2 key sections in three basins: Anglo-Paris Basin (Poigny core) (this study), Northern margin of Indian plate (Gongzha section, southern Tibet, China) (Li et al., 2017) and Western Interior Basin (USGS#1 Portland core, central Colorado; Iona-1 core, western Texas; Angus core, north-central Colorado) (Meyers et al., 2012b; Ma et al., 2014; Eldrett et al., 2015, Eldrett et al., 2017). Note that the CTB at Portland was placed through a fine lithostratigraphic correlation with the neighboring Turonian GSSP Pueblo section (Sageman et al., 1997). The onset and the end of CIE at Gongzha section were placed according to Li et al. (2017). The onset of CIE at Portland, Iona-1 and Angus cores was placed according to Sageman et al. (2006), Eldrett et al. (2015), and Joo and Sageman (2014) respectively. The end of CIE at Portland, Iona-1 and Angus cores was replaced in the present study (previous interpretations were also indicated in light blue horizontal bars, with two options SG1 and SG2 for Portland (Sageman et al., 2006). The position of the end of CIE, which marks the end of the recovery phase, is more obvious at Iona-1 core (see also Fig. 8). However, the onset of CIE at Iona-1 core seems misplaced; correlation with Portland core indicates that such position is very likely (Eldrett et al., 2015). The end of CIE in the WIB should be around Bentonite 'D' (see Portland record, see also correlation between Portland and Pueblo in Supplementary Fig. S2). Note that Bentonite 'D' at Iona-1 is stratigraphically much higher than the end of CIE; this remark has been also noted by Eldrett et al. (2015) (their fig. 9, Supplementary Fig. S2). (For interpretation of the references to colour in this figure legend, the reader is referred to the web version of this article.)

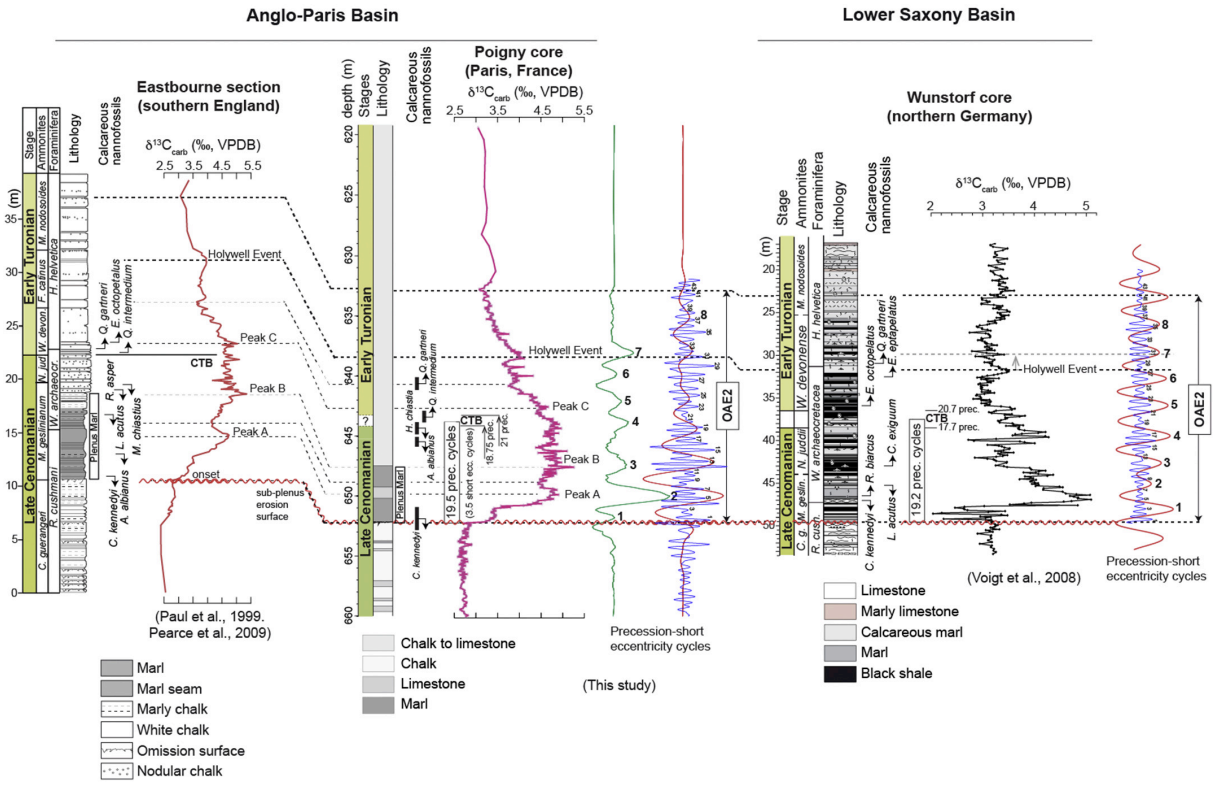

Fig. 5. Carbon-isotope and cyclostratigraphic OAE2 correlation between Eastbourne, Poigny and Wunstorf (Lower Saxony Basin). Cyclostratigraphic data of Eastbourne are from Gale (1995) and Gale et al., 1993, Gale et al., 1999, which are based on field interpretation. See also Fig. 6 and Supplementary Fig. S3 for a detailed cyclostratigraphic analysis based on $\delta^{13}C$ data. The onset of CIE is placed at the sharp lithological change in the three sections (Paul et al., 1999; Voigt et al., 2008). However, the end of CIE was placed at ~632 m at Poigny (see Fig. 2). At Wunstorf, we replaced the end of CIE at ~23.1 m instead of ~36 m (Voigt et al., 2008). Note that the ~23.1 m stratigraphic position marks the last black-shale bed, thus, the extent of OAE2 at Wunstorf as defined in the present study is equivalent to the Hesseltal Formation, i.e. corresponds to the extent of black shales. The end of CIE at Eastbourne could be placed by the projection into its lateral equivalent CIE at Poigny. Note that the Holywell Event at Wunstorf (Voigt et al., 2008) could be shifted upsection by a half short eccentricity cycle (indicated by an arrow) to match the short eccentricity cycle number 7, as in the Poigny record. Calcareous nannofossil data of Wunstorf core are from Linnert et al. (2010).

Table 1. Numbers of short eccentricity and precession cycles encompassing 'Perturbation' interval (from the onset of CIE to the CTB, see Section 4.2.1). Each given number is referred to the appropriate figure from which it is inferred.

Sections	Short eccentricity	Precession	References
Poigny	~3.5 (Fig. 2, Fig. 3)	~18.5 to ~21 (Fig. 2, Fig. 3)	Present study
Eastbourne	~3.5 (Fig. 6B)	~17.5 to ~18.5 (Fig. 6)	Present study
Wunstorf	~3.5 to ~4 (Fig. 5)	~18 to ~21 (Fig. 5)	Voigt et al. (2008)
Oued Bahloul	~3.25 (Fig. 7)	No data	Caron et al. (1999)
Portland/Pueblo	~5.5 (Fig. 4)	No data	Sageman et al. (2006)

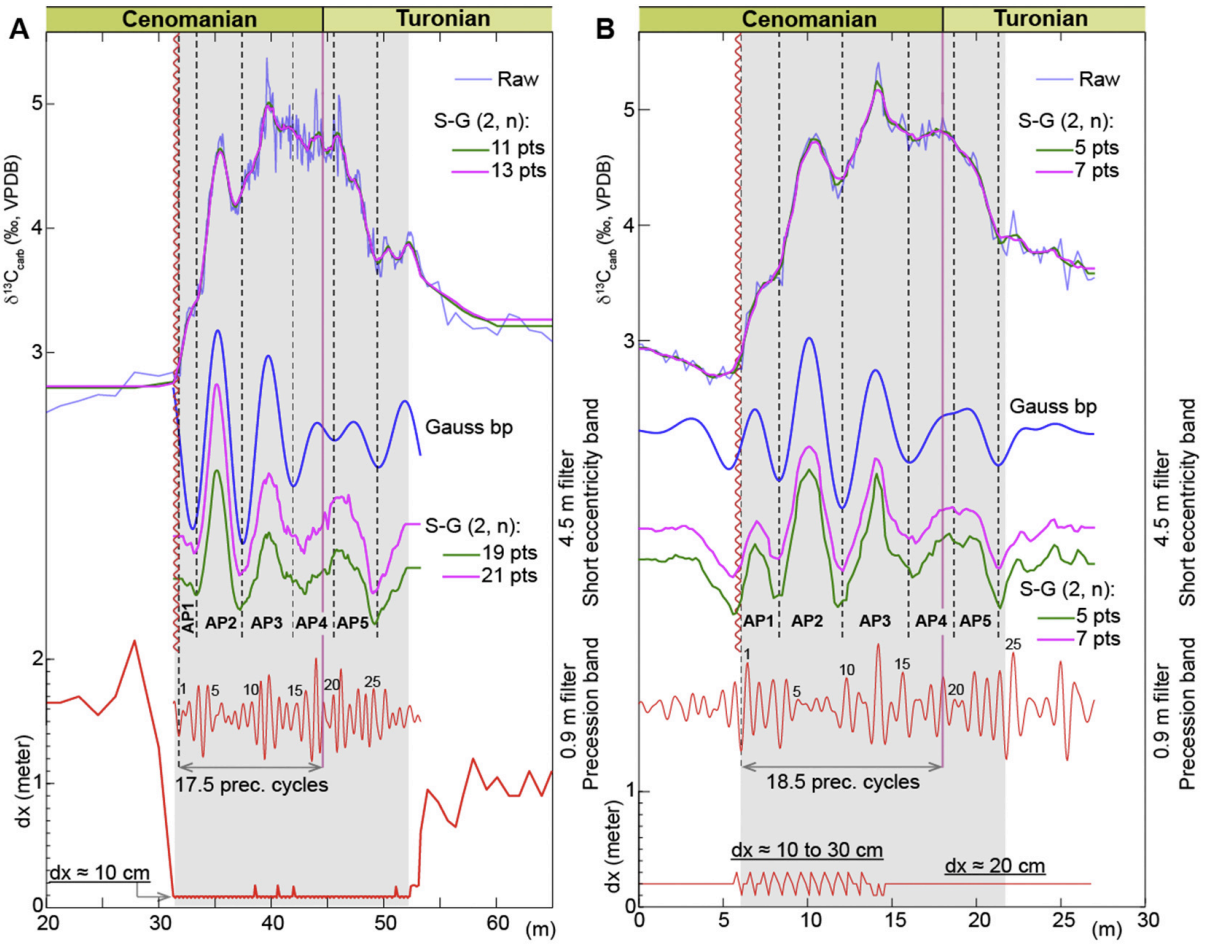

Fig. 6. Time-series analysis of bulk carbonate $\delta^{13}C$ data of the Eastbourne reference section (southern England). **(A)** Data are from Paul et al. (1999) and Jarvis et al. (2006). **(B)** Data are from Tsikos et al. (2004). Sampling steps (dx) of the two datasets are shown in the lowermost red curves. Same used time-series methods as in Fig. 2, Fig. 3. For the power spectra, see Supplementary Fig. S3. Short eccentricity Gauss bandpass (bp) is 0.22 ± 0.15 cycles/m, and precession Gauss bp is 1.1 ± 0.5 cycles/m. S-G filters at the short eccentricity band is applied to 30% weighted average (wa) detrend in 'A', and 25% wa detrend in 'B'. Grey-shaded area indicates the interval of highly resolved short eccentricity cycles AP1 through AP5 (see Fig. 2). Note that AP1, which is reduced in the Anglo-Paris Basin, is better resolved in Tsikos et al.'s (2004) data than in Paul et al.'s (1999) data. Number of precession (prec.) cycles from the onset of the CIE to the CTB is shown. (For interpretation of the references to colour in this figure legend, the reader is referred to the web version of this article.)

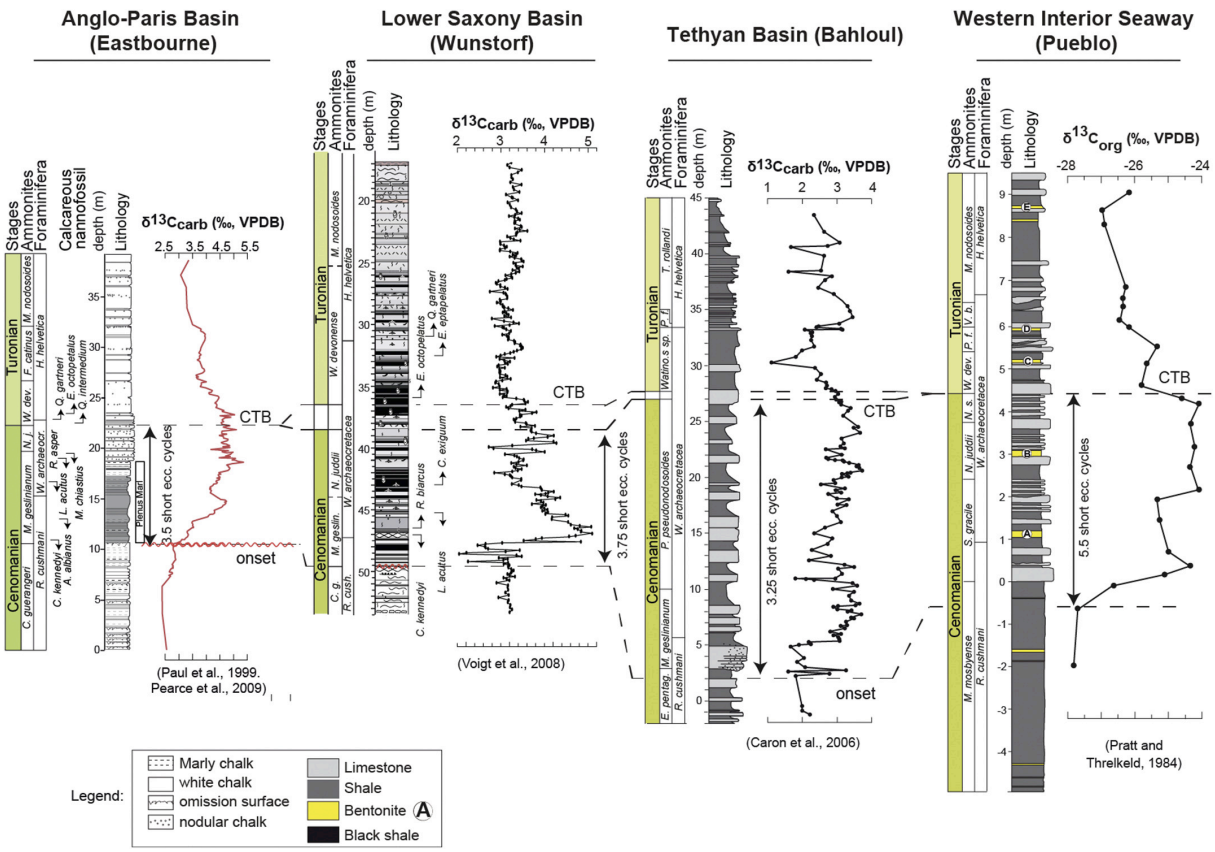

Fig. 7. Litho-biostratigraphy, and carbon-isotope ($\delta^{13}C$) stratigraphy of biostratigraphically (ammonites) dated sections in four sedimentary basins, Anglo-Paris Basin (Eastbourne section, Paul et al., 1999), the Lower Saxony Basin (Wunstorf core, Voigt et al., 2008), the southern Tethyan Basin (Oued Bahloul section, Tunisia, Caron et al., 2006), and the Western Interior Basin (Pueblo section, Pratt and Threlkeld, 1984). The CTB in the four sections was precisely defined on the basis of ammonites. Based on this definition, the interval from the onset of the CIE to the CTB contains three and a half (or 3.75) short eccentricity cycles at Eastbourne, 3.75 to 4.25 cycles at Wunstorf, and three and a small part of a fourth short eccentricity cycle at Oued Bahloul, against five and a half short eccentricity cycles at Pueblo.

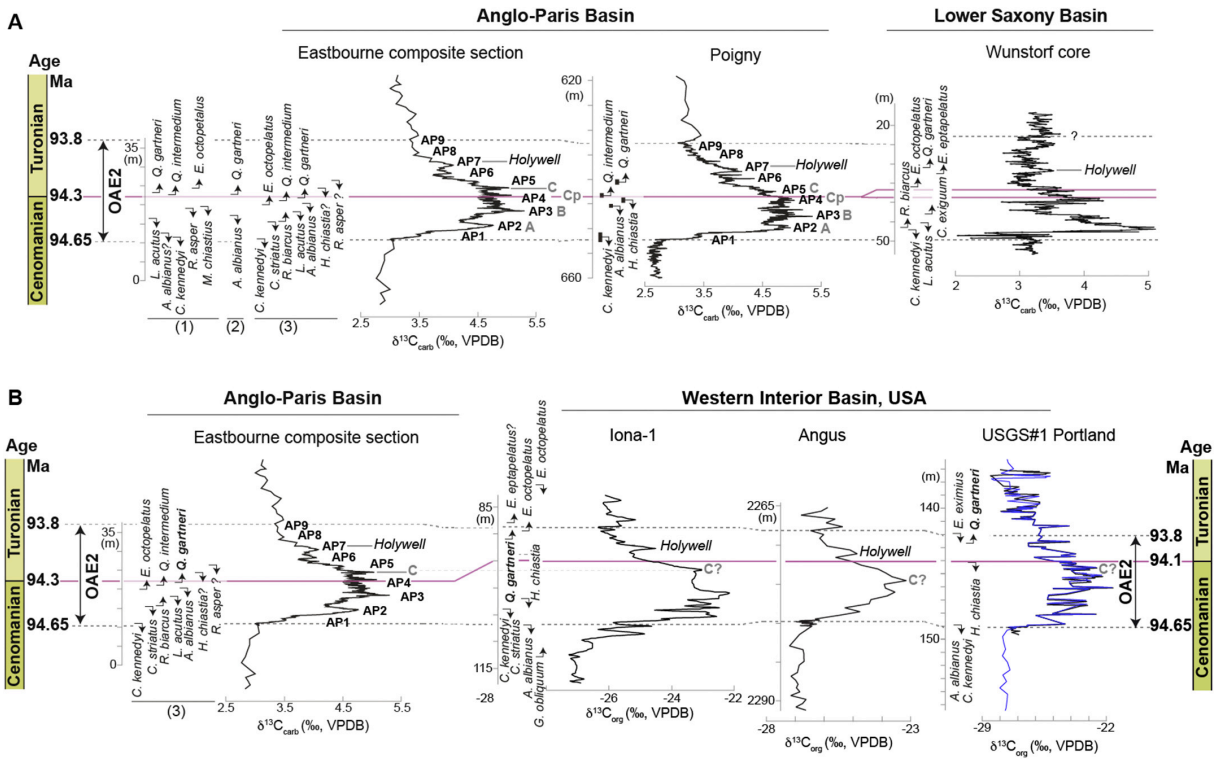

Fig. 8. Stable carbon-isotope ($\delta^{13}C$) and calcareous nannofossil correlation of OAE2 sections between the Anglo-Paris and Lower Saxony basins **(A)**, and between the Anglo-Paris and Western Interior basins **(B)**. $\delta^{13}C$ data of Eastbourne section (Sussex, southern England) are from Paul et al. (1999) with additional data points from Jarvis et al. (2006). $\delta^{13}C$ data of Poigny core (Paris, France) (this study). $\delta^{13}C$ data of Wunstorf core (northwestern Germany) are from Voigt et al. (2008). $\delta^{13}C$ data of Iona-1 core (western Texas, USA) are from Eldrett et al., 2015, Eldrett et al., 2017. $\delta^{13}C$ data of Angus core (north-central Colorado, USA) are from Joo and Sageman (2014). $\delta^{13}C$ data of USGS#1 Portland core (central Colorado, USA) are from Sageman et al., 2006). Note that the CTB at Portland was placed through a fine lithostratigraphic correlation with the Turonian GSSP Pueblo section (Sageman et al., 1997, see also Supplementary Fig. S2). AP1 through AP8 indicate location of $\delta^{13}C$ related short eccentricity cycles at Poigny (Fig. 2) and their possible lateral equivalents at Eastbourne (Abbreviation AP: Anglo-Paris). The age of CTB ranges from 93.90 ± 0.15 (Meyers et al., 2012b), 94.07 ± 0.15 and 94.10 ± 0.13 (Eldrett et al., 2015), and 94.12 ± 0.28 (Barker et al., 2011). Thus, we fixed it at 94.1 Ma (Eldrett et al., 2015) from the WIB. Then, three short eccentricity cycles above it till the end of CIE, and five and a half short eccentricity cycles below it till the onset of CIE were used according to USGS#1 Portland core cyclostratigraphy (Fig. 4, see Section 4.2.2). These two inferred ages of the onset and end of CIE (i.e., 94.65 and 93.8 Ma) were then projected into the Anglo-Paris Basin sections to infer a CTB age of 94.3 Ma there. For details on the onset and the end of the CIE, see Fig. 4, Fig. 5 and Supplementary Fig. S2.

References for calcareous nannofossil biostratigraphy are as follows:

Eastbourne section, (1) Paul et al. (1999), (2) Tsikos et al. (2004) and (3) Linnert et al. (2011); Poigny core (the present study); Wunstorf core: Linnert et al. (2010); Iona-1 core: Eldrett et al. (2015); USGS#1 Portland core: Bralower and Bergen (1998).

Supplementary Information

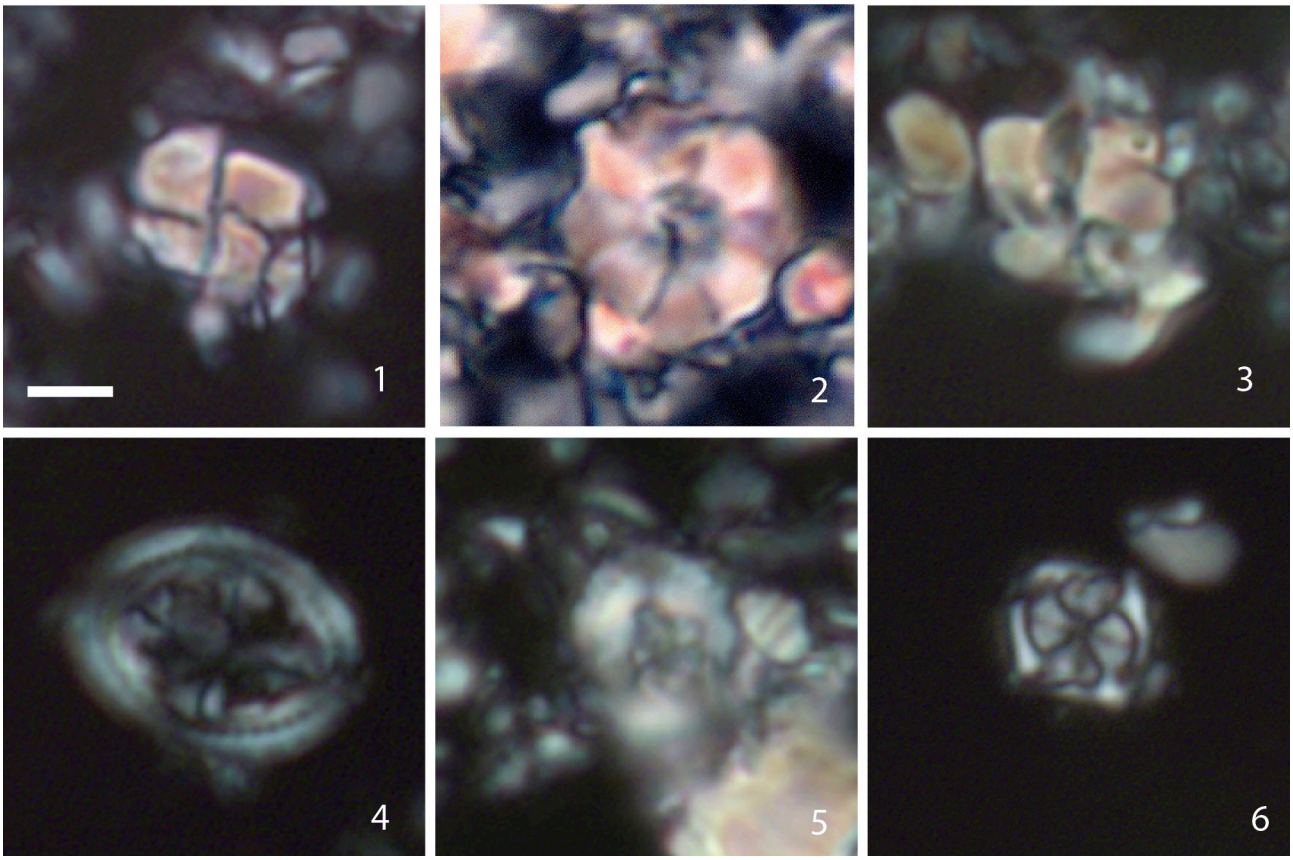

Plate S1: Micrographs of calcareous nannofossil species from Poigny core. All micrographs are under crossed nicols. Scale bar = 5 µm. All core depths of the corresponding samples are indicated in meter (m) between brackets. 1. *Quadrum gartneri* (depth 637.90 m), 2. *Eprolithus octopetalus* depth (638.90 m), 3. *Quadrum intermedium* (depth 644.90 m), 4. *Axopodorhabdus albianus* (depth 653.90 m), 5. *Helenea chiastia* (depth 648.90 m), 6. *Corollithion kennedyi* (depth 668.90 m).

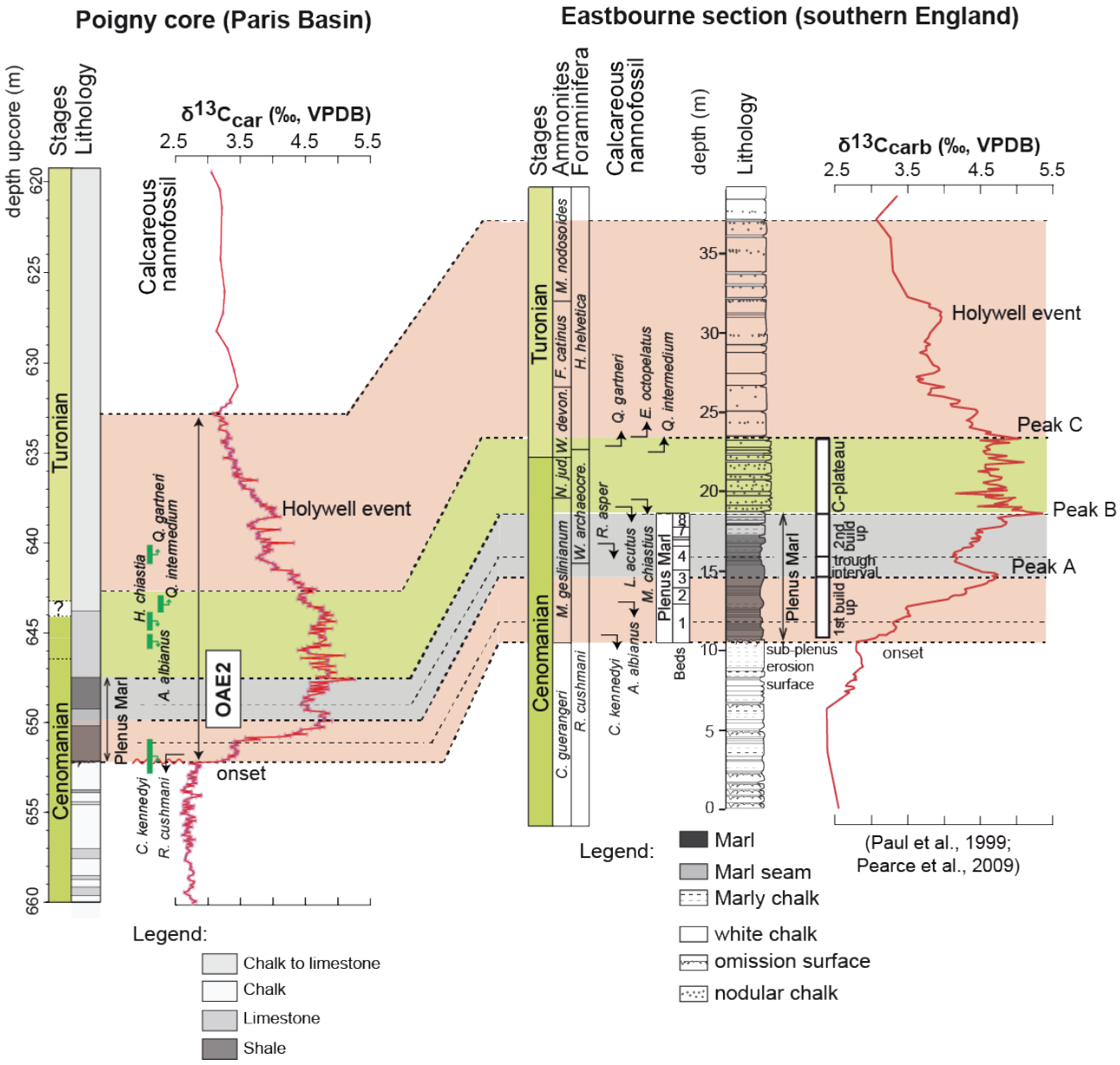

Figure S1: Litho-biostratigraphy and carbon-isotope ($\delta^{13}C$) data and correlation of the OAE2 interval between the Poigny core (this study) and the Eastbourne reference section (Paul et al., 1999; Jarvis et al., 2006).

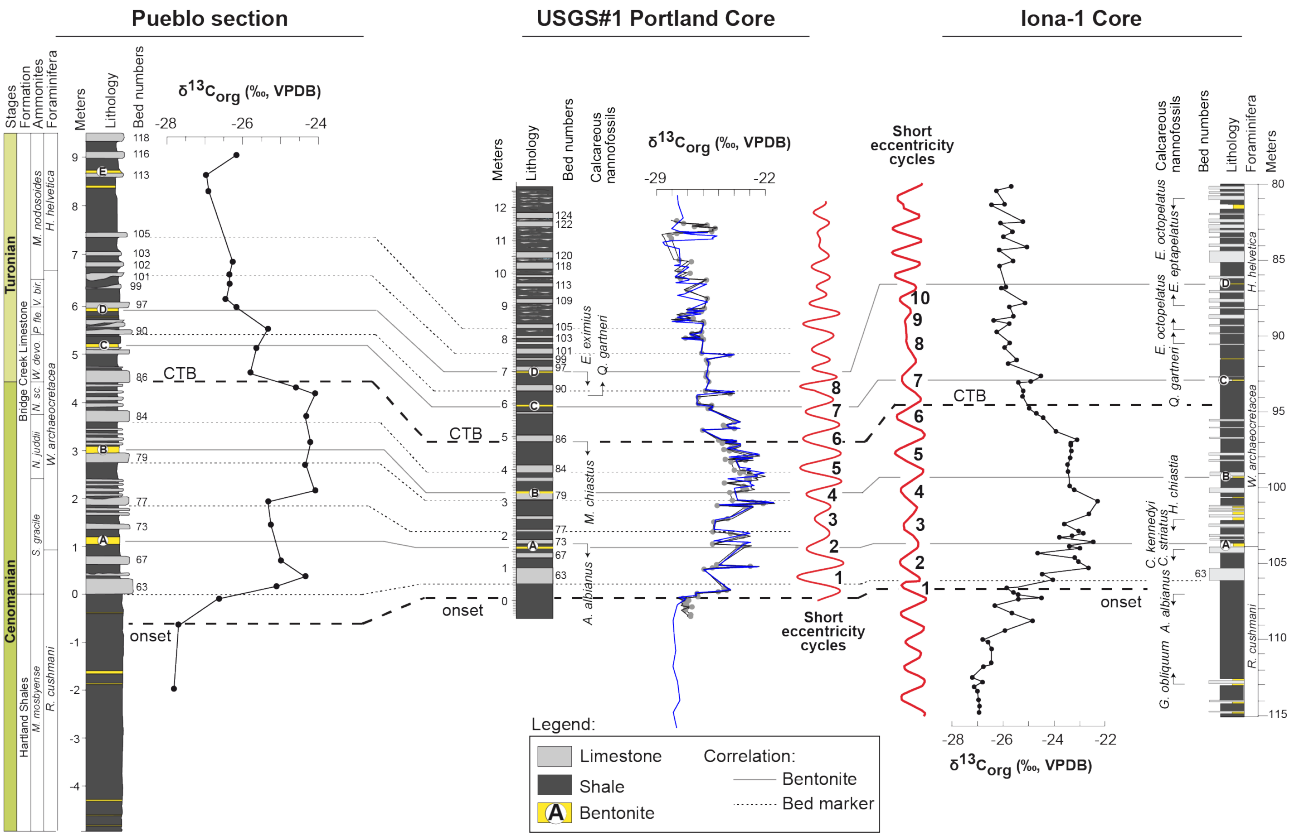

Figure S2: A detailed lithostratigraphic correlation (using bed markers) anchored at bentonite markers between the Pueblo section defined as the reference section of the Western Interior Basin (Turonian GSSP, Kennedy et al., 2005) and the USGS#1 Portland and Iona-1 cores. $\delta^{13}C$ data of Pueblo section (central Colorado, USA) are from Pratt and Threlkeld (1984). $\delta^{13}C$ data of USGS#1 Portland core (central Colorado, USA) are from Sageman et al. (2006) (grey curve) (additional data points to form the synthetic bleue curve of Joo and Sageman, 2014). $\delta^{13}C$ data of Iona-1 core (western Texas, USA) are from Eldrett et al. (2015, 2017). Cyclostratigraphic data of USGS#1 Portland and Iona-1 cores are from Sageman et al (2006) and Eldrett et al. (2015), respectively.

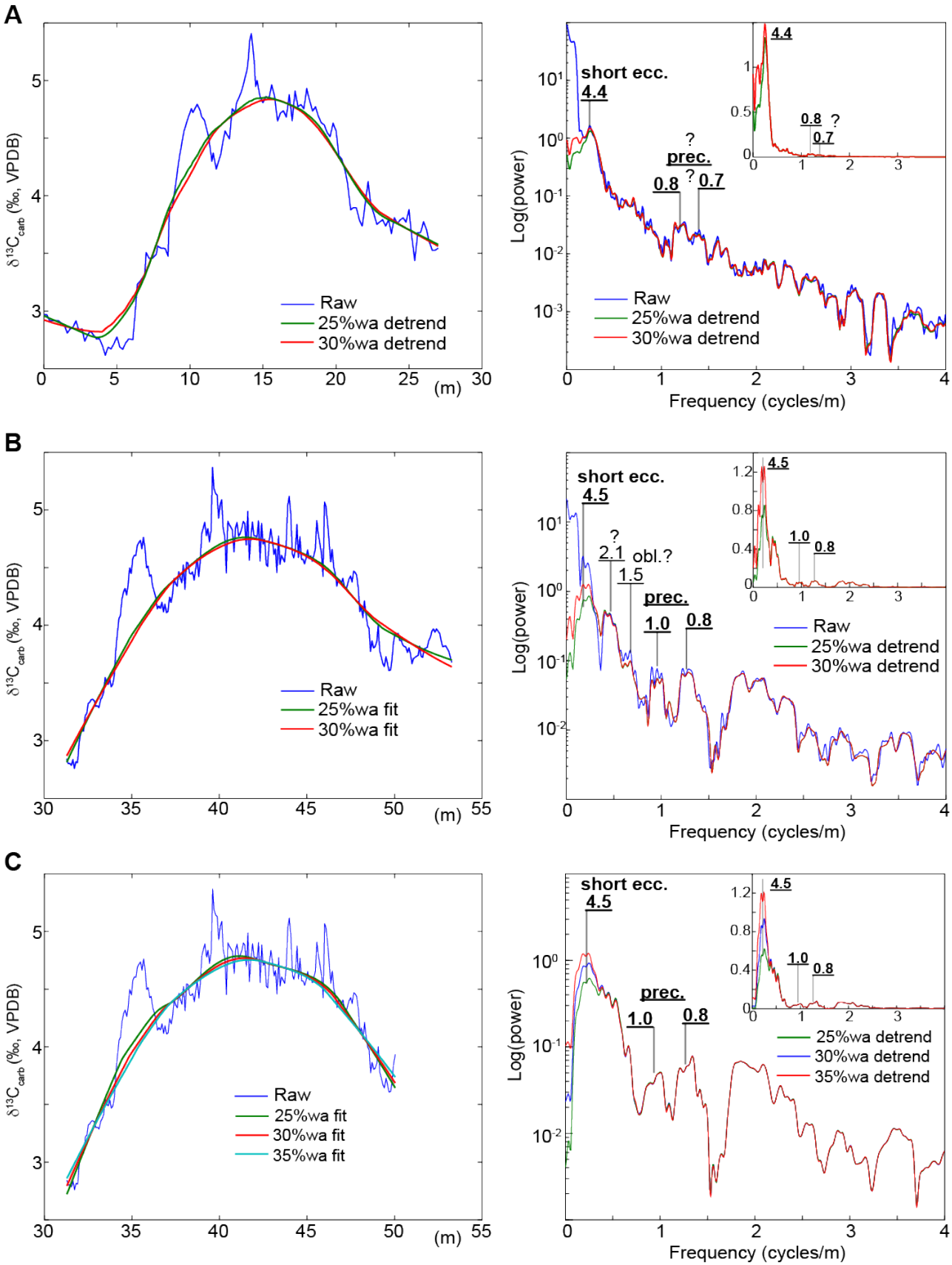

Figure S3: 2 π-MTM power spectra of bulk carbonate $d^{13}C$ data of Eastbourne section. Left panel for the raw $d^{13}C$ data along with weighted average (wa) fit, and the right panel for the power spectra in logarithmic and linear (*inset*) scales. **(A)** Tsikos et al.'s (2004) data. **(B)** Paul et al.'s (1999) data. **(C)** Paul et al.'s (1999) data excluding the uppermost part of the signal. Note that the uppermost part of

the signal records thinner short eccentricity cycles resulting in a 2.1 m peak in 'B' (compare spectra in 'B' and 'C'). Note that the ~4.5 m $d^{13}C$ related short eccentricity cycles are highlighted in the two datasets of Tsikos et al. (2004) and Paul et al. (1999). Precession cycle band could be retrived from Paul et al.'s (1999) $d^{13}C$ dataset. The stratigraphic resolution of $d^{13}C$ measurements are shown in the main Fig. 6.

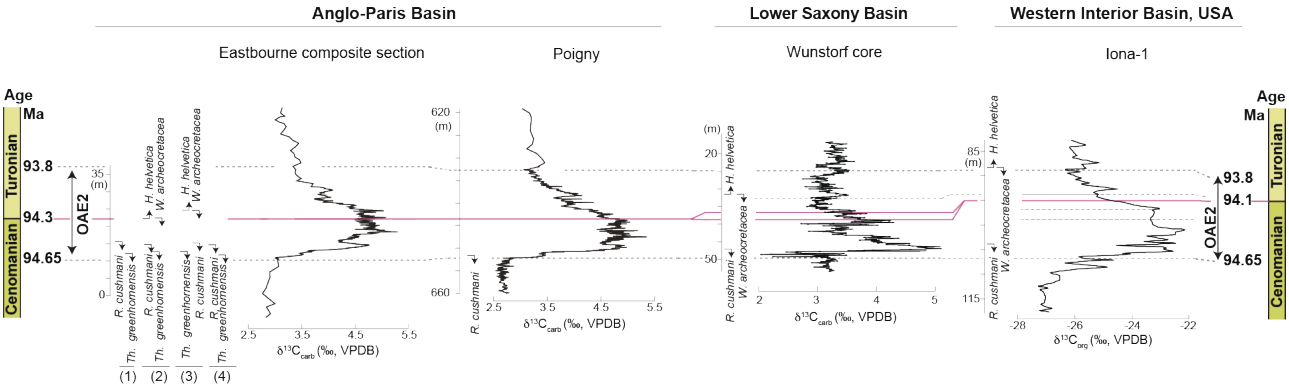

Figure S4: Stable carbon-isotope ($d^{13}C$) correlation between OAE2 sections from the Anglo-Paris, Lower Saxony and Western Interior Basins. $d^{13}C$ data of Eastbourne section (Sussex, southern England) are from Paul et al. (1999) and Jarvis et al. (2006). Data depicted by the gray curve are from the compilation of Jarvis et al. (2006). $d^{13}C$ data of Poigny core (Paris, France) (this study). $d^{13}C$ data of Wunstorf core (northern Germany) are from Voigt et al. (2008). $d^{13}C$ data of Iona-1 core (western Texas, USA) are from Eldrett et al. (2015, 2017). Planktonic foraminiferal bioevents of the Cenomanian-Turonian successions at Eastbourne after (1) Paul et al. (1999), (2) Keller et al. (2001), (3) Hart et al. (2002) and (4) Falzoni et al. (2018), at Poigny after Robaszynski and Bellier (2000), at Wunstorf core after Voigt et al. (2008), and Iona-1 core after Eldrett et al. (2015).

Additional reference:

Hart, M. B., Monteiro, J. F., Watkinson, M. P., Price, G. D., 2002. Correlation of events at the Cenomanian/Turonian boundary: Evidence from Southern England and Colorado. In: Wagreich, M. (Ed.), Aspects of Cretaceous Stratigraphy and Palaeobiogeography. Schriftenreihe der erdwissenschaftliche Kommission der Osterreichische Akademie der Wissenschaften, Wien, 15: 35–46, Verlag der Osterreichische Akademie der Wissenschaften, Wien.